Exchanges of sediment between the flood plain and channel of the Amazon River in Brazil

Thomas Dunne* *Donald Bren School of Environmental Science and Management, University of California, Santa Barbara, California 93106-5131*

Leal A. K. Mertes *Department of Geography* and *Institute for Computational Earth System Science, University of California, Santa Barbara, California 93106-4060*

Robert H. Meade *Water Resources Division, U.S. Geological Survey, Federal Center, Denver, Colorado 80225-0046*

Jeffrey E. Richey *School of Oceanography, University of Washington, Seattle, Washington 98195*

Bruce R. Forsberg *Instituto Nacional de Pesquisas da Amazônia, Manaus, AM Brazil*

ABSTRACT

Sediment transport through the Brazilian sector of the Amazon River valley, a distance of 2010 km, involves exchanges between the channel and the flood plain that in each direction exceed the annual flux of sediment out of the river at Óbidos (~1200 Mt yr^{-1}). The exchanges occur through bank erosion, bar deposition, settling from diffuse overbank flow, and sedimentation in flood-plain channels. We estimated the magnitude of these exchanges for each of 10 reaches of the valley, and combined them with calculations of sediment transport into and out of the reaches based on sediment sampling and flow records to define a sediment budget for each reach. Residuals in the sediment budget of a reach include errors of estimation and erosion or deposition within the channel. The annual supply of sediment entering the channel from bank erosion was estimated to average 1570 Mt yr^{-1} (1.3 × the Óbidos flux) and the amount transferred from channel transport to the bars (380 Mt yr^{-1}) and the flood plain (460 Mt yr^{-1} in channelized flow; 1230 Mt yr^{-1} in diffuse overbank flow) totaled 2070 Mt yr^{-1} (1.7 × the Óbidos flux). Thus, deposition on the bars and flood plain exceeded bank erosion by 500 Mt yr^{-1} over a 10–16 yr period. Sampling and calculation of sediment loads in the channel indicate a net accumulation in the valley floor of approximately 200 Mt yr^{-1} over 16 yr, crudely validating the process-based calculations of the sediment budget, which in turn illuminate the physical controls on each exchange process. Another 300–400 Mt yr^{-1} are deposited in a delta plain downstream of Óbidos. The components of the sediment budget reflect hydrologic characteristics of the valley floor and geomorphic characteristics of the channel and flood plain, which in turn are influenced by tectonic features of the Amazon structural trough.

INTRODUCTION

Sediments are exchanged between river channels and flood plains mainly through construction and destruction of the flood plain. Flood plains of large rivers are built by formation of bars and the accumulation of sediment carried in diffuse overbank flows and in channelized flows. They are destroyed largely by channel shifting and bank erosion. The rates of these processes can be quantified and compared with each other and with rates of downstream sediment transport to yield a comprehensive sediment budget for reaches. Previous studies of these processes have been concerned with the accumulation, destruction, or transport aspects, but rarely with all of them. In only a few studies (Kesel et al., 1992) have the full exchanges between constructive and destructive processes been evaluated and analyzed.

The rates at which sediment is transferred to and from flood plains, and the residence time of flood-plain storage, affect the maturation of mineral assemblages (Johnsson and Meade, 1990), the modulation of sediment-yield changes in response to land use (Trimble, 1983; Knox, 1987), and the routing of sediment through valley floors (Dietrich et al., 1982; Kelsey et al., 1987). The issue becomes particularly important because of the role of flood-plain sedimentation in sequestering and supplying bioactive chemicals such as carbon and pollutants (Marron, 1992; Lewin et al., 1977; Leenaers and Rang, 1989; Leenaers and Schouten, 1989; Graf, 1994).

Qualitative evidence that such exchanges can be large arises from direct field observations during floods, satellite images (Mertes, 1994), field surveys of sedimentation after floods (Gomez et al., 1995; Jacobson and Oberg, 1997), and stratigraphic studies of fluvial sedimentary environments (Reineck and Singh, 1980). Yet, despite abundant empirical and theoretical studies of sediment transport along rivers, resulting in the technical capacity to route sediment along channels, less attention has been paid to quantifying exchanges of sediment between channel and flood plain, and to understanding their controls. Kesel et al. (1992) systematized the analysis of these exchanges by quantifying a sediment budget for the lower Mississippi River and its flood plain before the era of extensive river modification. They compiled rates of river bank erosion, point-bar growth, and thalweg elevation change, and estimated the overbank sediment flux from mapping of deposit thicknesses.

In this paper we define the full range of exchanges of sediment between the channel and flood plain of a 2010 km reach of the Amazon River, Brazil. The reach is unaltered by engineering works that might inhibit natural exchange processes. Furthermore, we make our evaluation in the context of measured sediment transport in the river, so that the rates of exchange with the

*e-mail: tdunne@bren.ucsb.edu

GSA Bulletin; April 1998; v. 110; no. 4; p. 450–467; 10 figures; 3 tables.

flood plain can be compared with rates of channelized sediment transport.

The first systematic studies of channelized sediment transport in the Amazon River system were conducted by Sioli (1957) and Gibbs (1967), both of whom defined a general downstream decrease in sediment concentration along the main stem and emphasized the overwhelming influence of the Andes Mountains as the source of the river's load. Schmidt (1972) made the first detailed study of the annual cycle of surface sediment concentration at a station near Manaus. Meade et al. (1979, 1985) reported width- and depth-integrated measurements of suspended-sediment discharge, which led to the latest published estimate of the average annual sediment discharge at Óbidos of 1200 ± 200 Mt yr^{-1}.

To quantify the processes that transport sediment between the channel and the flood plain throughout the Brazilian Amazon, and to examine the controls on these processes over decadal time scales, we constructed a sediment budget for the channel and flood plain (Fig. 1) in 10 sampled reaches of the valley between São Paulo de Olivença and Óbidos, and an unsampled reach between Óbidos and the river mouth (Fig. 2). We measured sediment loads in the Amazon and its tributaries at gauging and other sampling stations (Table 1, Fig. 2) that bracket 10 reaches between São Paulo de Olivença, 740 km downstream of Iquitos, Peru (river km 740), and Óbidos (rkm 2750), and combined the results with flow records to define average annual fluxes through reaches averaging 200 km (146–280 km) in length. We then measured bank erosion and bar deposition rates, and calculated sediment transport into the flood plain by diffuse overbank flow and through flood-plain channels to complete the sediment budget for each reach. We extended our analysis 450 km farther downstream on the basis of sediment transport estimates in the coastal environment and an examination of valley-floor morphology in the reach between Óbidos and Almeirim. The annual sediment exchanges between the channel and the flood plain in the Brazilian reach of the Amazon alone are larger than the annual channel transport through the reach.

We have interpreted the processes responsible for the decadal-scale sediment budget of each reach in terms of the interactions between channel and valley-floor hydrology and the tectonically influenced pattern of channel and flood-plain characteristics described by Mertes et al. (1996). We present and interpret the sediment budget after first describing conditions that affect sediment transport through the valley floor. We conclude with a summary of the physical controls on channel–flood-plain exchanges of sediment in a large river.

DESCRIPTION OF THE AMAZON VALLEY

Geology and Sediment Sources

The Amazon rises in the Andean Cordillera, a region of high relief developed mainly in thinly bedded sedimentary and volcanic rocks. The combination of steep slopes and weak rocks favors channel incision, rapid mass wasting, and high sediment yields (Guyot, 1993). Erosion is accelerated by land use to an unknown degree, but from cursory field and aerial observations we judge this effect to be small relative to the high background rate of erosion in the Andes.

After leaving the Andean foothills, the tributaries of the Amazon cross the adjoining foreland basin where they deposit large volumes of sediment (Guyot, 1993; Räsänen et al., 1990), and then converge to flow along a downwarp filled with as much as 8000 m of sedimentary rocks ranging in age from Paleozoic to Tertiary (Petri and Fúlfaro, 1988; Nunn and Aires, 1988). A graben at the eastern end of the downwarp fixes the location of the river mouth. Two shields of Precambrian crystalline rocks flanking the trough are mainly regions of low relief and gentle gradients, mantled with deep saprolite and dense equatorial forest into which clearing and road building have made only local incursions. These shields have extremely low rates of erosion.

The rivers in the Amazon trough are bordered by a late Cenozoic plain having an area of approximately 90 000 km^2 between São Paulo de Olivença and Óbidos. The plain includes unconsolidated fluvial and lacustrine sands, silts, and clays, some of which constitute modern flood plains, and the remainder consists of terrace remnants of various ages and elevations. As the Amazon crosses three structural highs and the downstream end of a fault block that tilts the valley floor toward the south-southeast (Tricart, 1977), its flood-plain width decreases, constraining the sinuosity of the channel and increasing its gradient, as shown schematically in Figure 3 and in Mertes et al. (1996, Fig. 6), which includes measured values of flood-plain width and channel sinuosity.

Channel and Flood-Plain Form

The Amazon channel is remarkably straight in most of its Brazilian course; sinuosities of 100-km-long reaches average 1.0–1.2, except in a 350 km-long reach where sinuosities range from 1.3 to 1.7 (Mertes et al., 1996, Fig. 6). The channel has a wide floor, and bank gradients of approximately 0.2–1.0. Low-water widths, averaged over 100 km reaches, measured on 1:250 000 scale radar images, generally increase from 2 km near São Paulo de Olivença to more than 4 km near Óbidos, and similarly averaged low-water depths measured from navigation charts increase gradually from 10 to 20 m (Mertes et al., 1996, Fig. 4). However, gauging stations maintained by the Brazilian Departamento Nacional de Agua e Energia Elétrica and our own sampling stations are sited in reaches narrower and deeper than the average, as is typical in gauging practice. Bed material ranges from very fine to medium sand; median grain sizes at crossings average 0.31 mm (standard deviation = 0.09 mm) upstream of rkm 1500 (near Jutica) and 0.20 ($\pm$ 0.07) mm downstream (Nordin et al., 1980).

The river flows in a single channel throughout most of its course, although islands and bars of various sizes complicate the pattern. Smaller flood-plain channels, having a wide range of widths and depths, diverge from and rejoin the main channel after excursions of a few kilometers to more than 100 km across the flood plain. Although there are thousands of channels on the flood plain, in this paper we consider only those flood-plain channels that are connected directly to the mainstem and are able to convey water and sediment from it. Other channels on the flood plain are fed by local rainfall or by runoff from the forested craton, and they carry little or no sediment.

The flood plain is highly complex (Mertes et al., 1996). Between São Paulo de Olivença and Itapeua, it is dominated by scroll-bar topography and hundreds of narrow, crescentic lakes. Between Itapeua and São José do Amatarí, the flood plain is narrow and has few lakes and little evidence of channel migration. Downstream of São José do Amatarí a relatively low and incomplete levee system breached by large distributary channels allows inundation of a wide flood plain containing lakes of roughly equant shape and irregular outlines that appear to be due to subsidence of compacting sediment. Seasonal patterns of flood-plain–channel exchanges of water were described by Richey et al. (1989b).

Channel Gradient

Channel gradient is an important characteristic affecting sediment transport and channel behavior in rivers, but the gradient of the Amazon has not been surveyed. We have calculated water-surface gradients from satellite measurements of elevation (see Fig. 3B and caption for explanation). The gradients were obtained at low water, and thus are taken as a close approximation of average channel-bed slope. The horizontal bars in Figure 3B indicate average channel-bed slopes over the distances between satellite crossings. They generally decrease downstream, but in four reaches there is a steepening followed by a de-

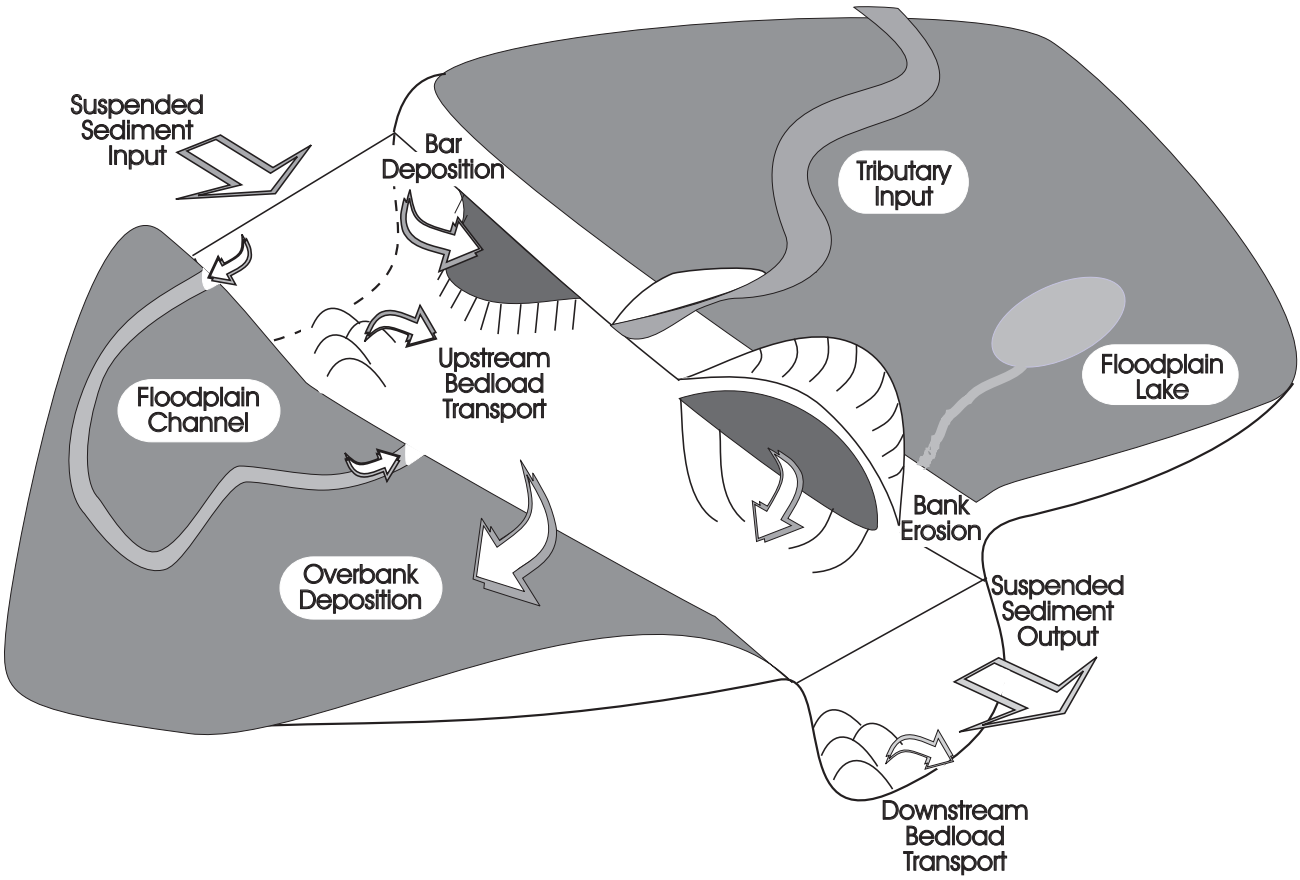

Figure 1. Processes governing the sediment budget of a channel–flood-plain reach. Sediment enters a reach of channel: (1) from upstream; (2) from tributaries within the reach; and (3) from bank erosion. It leaves the reach by: (1) channel transport; (2) deposition on bars; (3) diffuse overbank flow; and (4) through flood-plain channels.

cline of gradient. Although the gradient changes can be located only approximately because of the positioning of the satellite passes, three of these changes are associated with structural highs crossed by the river (the Jutaí arch, the Purús arch, and the Monte Alegre intrusion) referred to by Caputo (1984, Fig. 18) and by Petri and Fúlfaro (1988, Fig. I-4). The structures are located only approximately from small-scale maps and are probably broader than the bars in the figure. The most rapid decrease in gradient occurs downstream of the Purús arch, at the confluence of the structurally controlled valley of the River Negro and the elongate east-northeast–trending Amazonas structural basin (Sternberg, 1955; Tricart, 1977; Caputo, 1984, p. 168 and following). The Quaternary flood plain is wide between three structural highs, and relatively narrow where it crosses them (Fig. 3). Measured values of flood-plain width (Mertes et al., 1996, Fig. 6) are inversely correlated with channel gradient ($n = 15$; $\alpha < 0.06$) for the reaches outside the tilted fault block (labeled TFB in Fig. 3). Narrowing of the flood plain constrains channel sinuosity as the river impinges on cohesive banks, and the decrease in sinuosity increases the channel gradient. The fourth zone of increased gradient is in the vicinity of rkm 1000–1400 where the Amazon appears to have been shortened by autocapture and steepened as a result of faulting that tilted the valley floor to the south-southeast (Tricart, 1977, p. 8). The gradient then declines in the reach between rkm 1400 and Itapeua (rkm 1704) as the river flows along the southern margin of its valley away from the tilted reach.

We also estimated the water-surface gradient at various seasons of the year from 1400 vertical velocity profiles measured at five stations gauged regularly by the Departamento Nacional de Agua e Energia Elétrica and at two stations studied briefly by U.S. Geological Survey personnel. The results confirm the values of channel-bed slope in Figure 3B at low water, and demonstrate that upstream of Manaus surface gradients are approximately twice as great during rising water as those during falling water because of the passage of the annual flood wave. By contrast, at Óbidos water-surface gradients are lower during rising water and approximately twice as steep on the falling limb of the hydrograph because of the offset in the seasonal influx of water from the River Negro and River Madeira, as Meade et al. (1985) interpreted from records of stage at Manacapurú and Óbidos. Seasonal variations in water-surface slope are used in our estimates of water and sediment export to flood-plain channels.

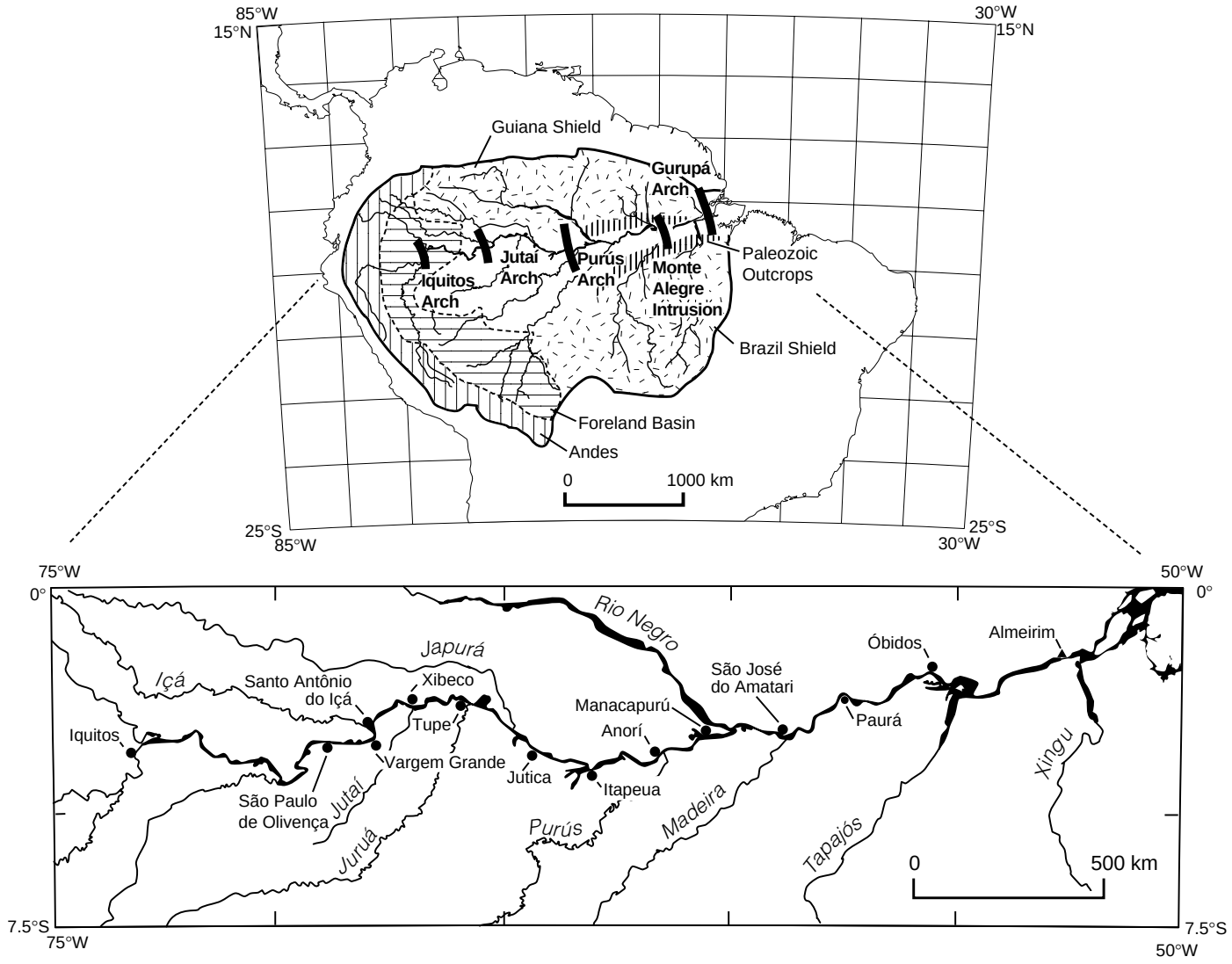

Figure 2. Map of the Amazon basin showing lithological regions and structural features, the major tributaries, and sampling stations (dots). The map contains one structural high, the Monte Alegre intrusion, not included in a similar map presented by Mertes et al. (1996). The geological literature of Brazil contains some differences of interpretation concerning the Purús arch and the Monte Alegre ridge. The term "arch" is usually confined to highs that involve flexure or faulting, whereas the term "alto" (high) is reserved for a feature not necessarily related to deformation, such as a topographic remnant or an intrusion. However, both the Purús and Monte Alegre features are referred to as "arches" in some literature. The Monte Alegre feature, for example, brings Paleozoic sandstones to the surface of the Amazon valley, where thick sequences of Cenozoic sediments outcrop.

SEDIMENT BUDGET OF THE RIVER CHANNEL

To understand the exchanges and transport of sediment along the Amazon, we calculated a mass balance (Fig. 1) for both silt-clay and sand in each of 10 reaches as follows:

$$Q_u + \sum_i Q_{trib_i} + E_{bk} = Q_d + D_{bar} + D_{ovrbk} + D_{fpc} + A_c \rho_b \frac{\Delta z}{\Delta t} \quad (1)$$

where Q_u, Q_d, and Q_{trib} are, respectively, the annual fluxes of suspended and bedload sediment at the upstream and downstream ends of each reach and from tributaries entering the reach; E_{bk} is bank erosion; D_{bar} is deposition on bars within and adjacent to the channel; D_{ovrbk} is deposition overbank; D_{fpc} is deposition in flood-plain channels; A_c (m^2) and Δz (m) are, respectively, the area and average elevation change of the main channel bed and banks in the reach; Δt is the time interval of the computation (yr), and ρ_b is the bulk density of the bed material (1.7×10^{-6} Mt m^{-3}). Each of the terms in equation 1 has units of Mt yr^{-1}. The entire budget is summarized in Figure 4, which combines inputs and outputs of channel sediment transport into a "net channel transport." The final term in equation 1 represents the rate of change of channel storage, but because it was determined as a residual, it contains all errors in the other terms, and therefore is indicated by the open rectangles and lines in Figure 4. In the following discussion, we elucidate the processes represented by each of the

TABLE 1. DRAINAGE BASIN AND FLOW CHARACTERISTICS AT SAMPLING STATIONS

Station	Distance downstream of Iquitos, Peru (river km)	Drainage area* ($km^2 \times 10^{-3}$)	Mean annual discharge† ($m^3s^{-1} \times 10^{-3}$)	Mean annual flood† ($m^3s^{-1} \times 10^{-3}$)	Bankfull discharge** ($m^3s^{-1} \times 10^{-3}$)
Mainstem					
São Paulo de Olivença (SPO)§	740	940	45.6	64	
Vargem Grande#	863	950	48.1	69	
Santo Antônio do Içá (SAI)§	891	1100	55.6	76	75
Xibeco (XIB)	1051	1115	56.0	78	
Tupé (TUP)	1248	1180	60.7	84	
Jutica (JUT)	1528	1700	63.2	103	
Itapeua (ITA)§	1704	1760	85.8	108	96
Anorí (ANO)	1885	1790	86.9	111	
Manacapurú (MAN)§	2031	2180	101.4	133	120
São José do Amatarí (SJA)	2248	2900	98.2	134	
Paurá (PAU)	2474	4340	154.7	227	
Óbidos (OBI)§	2750	4640	170.1	237	200–230
Tributaries§					
River Içá	890	108	7.1	10.0	
River Jutaí	1100	53	4.0	5.9	
River Juruá	1280	186	4.9	8.6	
River Japurá	1480	245	14.0	21.1	
River Purús	1910	358	11.1	19.2	
River Negro	2120	691	29.6	59.2	
River Madeira	2300	1336	29.3	54.2	

*Based on Digital Chart of the World and Radambrasil 1:1 million scale maps.
†Based on 16 years of record at the DNAEE gauging stations (occasional years of missing data) and on flood routing computations at sampling sites located between gauging stations.
§Gauging station maintained by the Brazilian Departamento Nacional de Agua e Energia Elétrica (DNAEE).
#Station used for sampling sediment concentrations which were combined with flow records from SPO to compute sediment discharge.
**Estimates of bankfull discharge are based on field observations of the onset of overbank flow.

terms, and describe how we estimated the quantities of sediment involved.

Calculation of Bedload

In the absence of measurements, we calculated bedload with the Yalin (1963) formula, which performs well for saltating sandy bed material when the local effective shear stress is used together with the fraction of the bed material that is not fully suspendible (Dietrich, 1982). After making extensive computations, including the use of local effective shear stresses based on hundreds of logarithmic flow-velocity profiles obtained by the Departamento Nacional de Agua e Energia Elétrica during their gauging program, and bed material textures given by Nordin et al. (1980) and by Mertes and Meade (1985), we concluded that maximum rates of bedload transport ranged from 0.01 to 0.05 Mt day^{-1}, or only about 1% of the suspended transport rate (Mertes, 1985). These values are well within the errors of measurement of suspended loads in the Amazon, and thus were ignored in the sediment budget.

Suspended Sediment Transport

We sampled sediment concentrations on various parts of the hydrograph to produce sediment-rating curves, and combined these curves with flow records for water years 1974–1989 to calculate annual fluxes. We collected width- and depth-integrated samples at 11 mainstem stations and at the mouths of 7 major tributaries between Vargem Grande and Óbidos (Table 1) approximately every 4 months during 1981–1984 and on single dates in 1988, 1990, and 1991. Sampling methods and processing were described by Meade (1985) and Richey et al. (1986).

On each cruise we sampled a different part of the annual flood wave. The boat traveled down the 2000 km reach at an average speed of approximately 100 km day^{-1}; the local water speed at the sampling sites was 90–190 km day^{-1}. Where possible, each sampling station was located at or near a gauging station maintained by the Departamento Nacional de Agua e Energia Elétrica. Stream flow and water level at sampling stations not gauged by the Departamento were calculated from gauged values at upstream and tributary stations with the Muskingum flood routing procedure described by Richey et al. (1989b). We updated the routing scheme by incorporating an improved estimate of unmeasured lateral inflow based on monthly rainfall maps for the ungauged tributary and flood-plain areas.

Sediment concentrations were analyzed separately for silt-clay (<0.06 mm) and sand. In the mainstem, total concentration ranged from 216–606 mg l^{-1} at Vargem Grande to 72–386 mg l^{-1} at Óbidos. Concentrations ranged from 1–10 mg l^{-1} in the River Negro, which drains only the forested craton, to 64–891 mg l^{-1} in the River Madeira, which drains the Bolivian Andes. Sediment-rating curves for silt-clay (<0.06 mm) and sand were constructed by regressing concentration against discharge and its rate of change using a significance level of 0.05. Most rating curves were looped when concentration was plotted against discharge; rising limb concentrations were as much as 2.5 times greater during rising water than at the same discharge during recession, and they began to decrease before the time of peak flow.

The rating curves for main channel and tributary stations were combined with records of mean daily flow for the water years 1974–1989, either from the Departamento Nacional de Agua e Energia Elétrica gauging stations or from flood-routing computations at intermediate main channel stations, to calculate daily and average annual fluxes of the two sediment classes (Table 2). An error-propagation analysis (Bevington, 1969) indicates that the standard error of the uncertainty around the long-term average annual sediment fluxes was approximately 9% at São Paulo de Olivença and 12% at Óbidos, because of the smoothness and regularity of the hydrograph, which facilitated sampling and minimized extrapolation. Analogous values for the tributaries were 11%–20%.

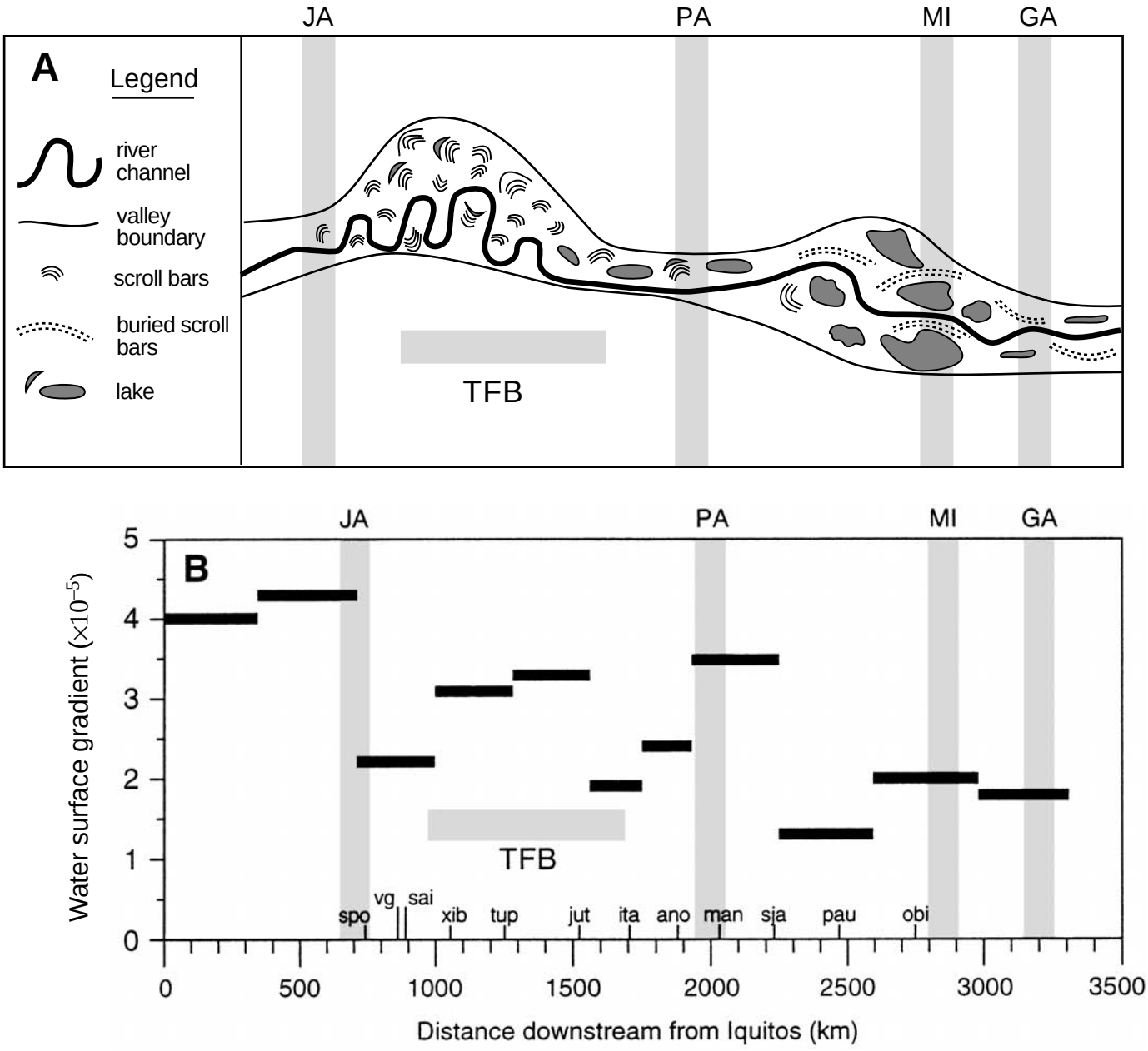

Figure 3. (A) Schematic illustration of the relations between geomorphic and structural features of the Amazon valley. The four vertical bars indicate the approximate locations of the axes of arches and buried bedrock ridges mapped by Petri and Fúlfaro (1988) and Caputo (1991): JA—Jutaí arch; PA—Purús arch (or ridge); MI—Monte Alegre intrusion and ridge; GA—Gurupá arch, respectively centered at approximately 700, 2000, 2840, and 3200 km downstream of Iquitos, Peru. TFB—the site of a tilted fault block proposed by Tricart (1977), extending from approximately 1050 to 1700 km downstream of Iquitos. (B) Water-surface gradient at low flow along a 3200-km-long reach of the Amazon River, based on radar altimeter measurements of water-surface elevation. Guzkowska et al. (1990) reported water-surface elevations extracted from Seasat radar data collected during low water between July 27 and August 9, 1978 for 32 sites along the mainstem of the Amazon River ranging from the coast inland to Peru. The precision was estimated to be within tens of centimeters, causing an uncertainty of ~1×10^{-6} in computed gradients. (The absolute accuracy of the elevation measurements also depends on the geoid model invoked, which results in ±1 m accuracy for absolute elevations, but our calculations of elevation differences should not be significantly affected by this uncertainty.) We replotted the orbit paths for the data reported by Guzkowska et al. (1990) on 1:250 000 scale maps for the Brazilian sites (Radambrasil, 1972). The altimetric results listed by Guzkowska et al. (1990) as having the lowest accuracy were not included. Orbits with multiple river crossings were also excluded, leaving 12 elevations from which gradients were calculated. The corrected river distances were combined with the elevation data to calculate water-surface gradients. Each horizontal bar indicates the average gradient for a reach between adjacent satellite crossings. Although the radar data were collected over a two week period, the graph represents a synoptic view of the water-surface gradient at low water, because the change in the gauged height of the river at the five mainstem gauging stations was less than 1 m during this time. Abbreviations on the abcissa: spo—São Paulo de Olivença; vg—Vargem Grande; sai—Santo Antônio do Içá; xib—Xibeco; tup—Tupé; jut—Jutica; ita—Itapeua; ano—Anorí; man—Manacapurú; sja—São José do Amatarí; pau—Paurá; obi—Óbidos.

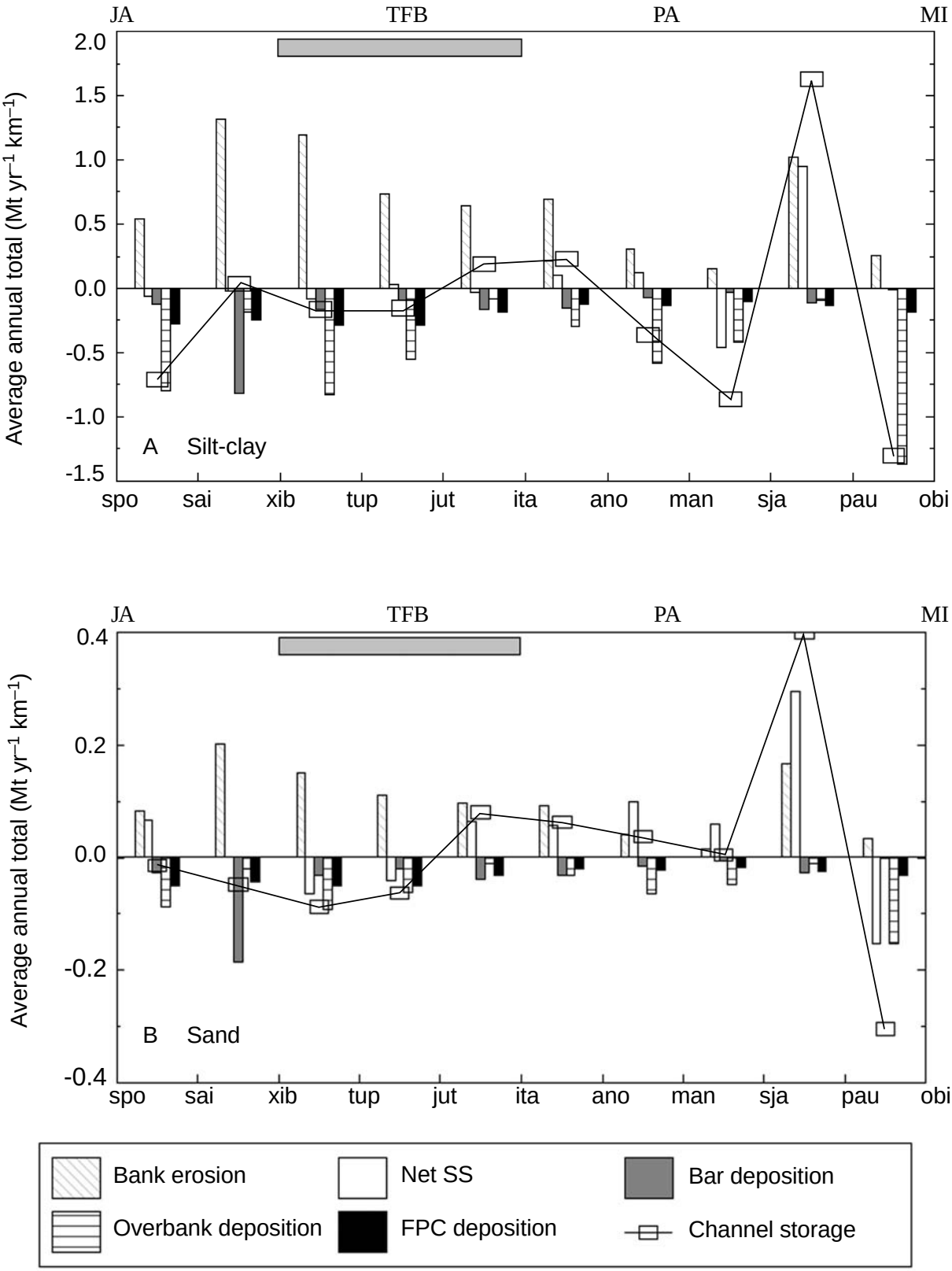

Figure 4. Summary of the sediment budget of the channel in each reach during water years 1974–1989. (A) Silt-clay. (B) Sand. Positive values indicate sediment supplied to the channel; negative values indicate transfers from the channel to the flood plain or to downstream transport. Each term is normalized by the length of the respective reach. Note the difference in ordinate scales. Abbreviations as in Figure 3.

TABLE 2. MEAN ANNUAL SEDIMENT FLUX RATES (MT YR^{-1}) FOR ALL STATIONS IN DOWNSTREAM ORDER FOR 1974–1989

Station	Sand		Silt-clay		Sand (%)
São Paulo de Olivença*	143	(18)	473	(40)	23
River Içá†	5	(1.5)	19	(3)	22
Santo Antonio do Içá	141	(11)	501	(60)	22
River Jutaí	0.2	(0.3)	2	(0.1)	9
Xibeco	141	(10)	505	(55)	22
Tupé	154	(19)	524	(47)	22
River Juruá§	5	(1.2)	23	(4.4)	18
River Japurá#	6	(1.7)	24	(1.5)	17
Jutica	177	(14)	561	(62)	20
Itapeua	164	(11)	567	(43)	23
Anorí	157	(11)	549	(55)	22
River Purús	2	(0.6)	23	(4.5)	8
Manacapurú	142	(7)	555	(38)	20
River Negro	0.5	(0.1)	7	(0.7)	7
São José	131	(10)	652	(51)	17
River Madeira**	144	(36)	571	(87)	20
Paurá	206	(25)	991	(155)	18
Óbidos	248	(17)	991	(129)	20

Notes: The values in parentheses are the standard errors, obtained through an error propagation analysis of the sediment rating curves and flow records.

*Sediment rating curve from Vargem Grande combined with flow record from SPO.

†13 yr average, without 1981,1985,1986.

§15 yr average, without 1982.

#15 yr average, without 1981.

**15 yr average, without 1989.

Net Channel Transport

The terms Q_u, Q_d, and Q_{trib} were calculated for each reach and year during 1974–1989 from the sediment rating curves and flow records. Their sum ($Q_u + \Sigma Q_{trib} - Q_d$), the net change in channel transport for each reach, is plotted in Figure 5. Despite the fact that these values represent differences between much larger numbers, and upstream of Manacapurú are only 1%–5% of the flux through the reach for silt-clay and 4%–10% for sand, the annual values in most reaches show remarkable interannual consistency over the 16 yr when the high flows at Manaus varied over almost the entire range recorded between 1902 and 1996 (Richey et al., 1989a). Net changes in transport downstream of Manacapurú constitute much larger fractions of the load. For example, between São José do Amatarí and Óbidos, 30% of the silt-clay and 21% of the sand transported into the 502-km-long reach do not leave it. However, the interannual consistency of computed sediment transport simply reflects the low variability of annual flows, which have a coefficient of variation of only 7%–10% at stations along the main channel.

An error-propagation analysis (Bevington, 1969) of the effects arising from uncertainty in the sediment rating curves, based on the assumption that uncertainties in the inputs and outputs of each reach were uncorrelated, yields maximum standard errors for the net silt-clay flux that range from 70 to 80 Mt yr^{-1} for reaches upstream of Itapeua, declining downstream to 64 Mt yr^{-1} in the Manacapurú–São José do Amatarí reach, and then rising to 180–200 Mt yr^{-1} downstream of São José do Amatarí. The standard errors for the net sand flux were 20–23 Mt yr^{-1} upstream of Jutica, declining to 12 Mt yr^{-1} in the Manacapurú–São José do Amatarí reach, and rising to 30–45 Mt yr^{-1} downstream of São José do Amatarí and the River Madeira. Thus, the computed changes in silt-clay are only statistically significant for the reaches between Manacapurú and Paurá, but the changes in sand transport (positive or negative) for most reaches are greater than or close to the limits of detection.

Change in silt-clay transport shows no consistent spatial pattern upstream of Itapeua (Fig. 5A). Downstream, there is a general pattern of accumulation, but it is interrupted by one large, anomalous increase in silt-clay transport in the Manacapurú–São José do Amatarí reach (averaging 91 Mt yr^{-1}, or 462 000 t yr^{-1} km^{-1} of channel), despite the abrupt decrease in channel gradient on the downstream side of the Purús Arch (Fig. 3). This apparent anomaly is associated with a large influx of sediment-free water from the River Negro and from an extensive area of ungauged small tributaries and flood plain. The inflow is particularly large from the north side of the valley, and it can be seen on Landsat images to confine sediment-rich water to the south side of the channel and flood plain. The flood plain in this reach exhibits fields of exposed sand and a relatively low proportion of silt-clay in the sediments (Mertes et al., 1996, Fig. 5).

In the São José do Amatarí–Paurá reach, there is massive loss of silt-clay from transport (positive values in Fig. 5A) where the River Madeira supplies the largest tributary source of sediment in the entire study reach. The Paurá-Óbidos reach exhibits interannual variations in net silt-clay transport, the magnitudes of which are correlated with the ratio of the annual flows from the two large tributaries (Fig. 6). Relatively high discharges from the River Madeira result in accumulation of silt-clay, whereas relatively high flows from the sediment-poor River Negro cause net removal of fine sediment from the Paurá-Óbidos reach.

There is a net increase in sand transport from Santo Antônio do Içá to Jutica as the river gradient increases, and then net loss of sand from transport begins at Jutica as the gradient begins to decline (Fig. 5B). Unfortunately, it is not possible to locate more precisely the onset of the gradient reversal between Tupé and Jutica because of the spacing of the available satellite orbits used for Figure 3B. The calculated changes in channel transport upstream of Anorí do not exceed the standard errors for this quantity, but they are included in this discussion as hypotheses because the error-propagation technique maximizes uncertainty in the standard errors of the computed changes. The trend appears to be one of accumulation in the São Paulo de Olivença–Santo Antônio do Içá reach, followed progressively by scour as the gradient increases downstream between Santo Antônio do Içá and Jutica (rkm 1528), and then a gradual return to accumulation downstream. The only reaches in which there is a net addition of sand to channel transport (negative values on the graph) are (1) between Xibeco and Jutica, where gradients increase downstream in response to neotectonic tilting, and (2) between Paurá and Óbidos, where channel gradient increases slightly as the flood plain narrows in approaching the Monte Alegre intrusion (Fig. 3; Mertes et al., 1996, Fig. 6). Sand accumulates even in the Manacapurú–São José do Amatarí reach from which silt-clay is scoured, indicating that for sand the effect of decreasing gradient is not offset by the flushing action of sediment-poor water from the craton. Decrease in transport of sandy bed material in that reach is consistent with the formation of island bars; 70% of the channel change in this reach is due to island change (Mertes et al., 1996, Fig. 8).

Bank Erosion and Bar Deposition

Estimates of the contribution of flood-plain sediments to the channel sediment load from bank erosion (E_{bk}) and loss of sediment due to bar dep-

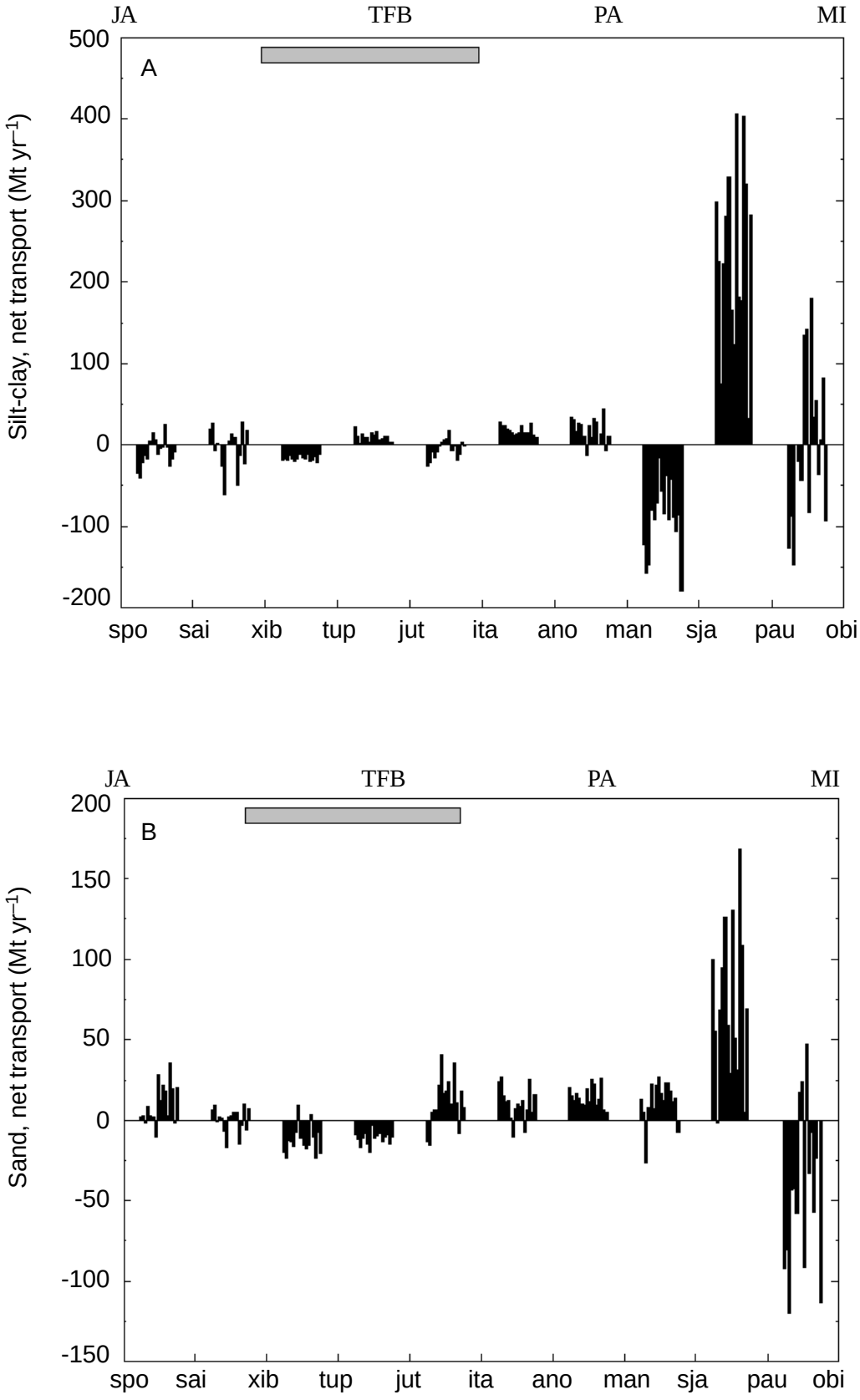

Figure 5. Net suspended sediment transport for each reach and for each year 1974–1989. (A) Silt-clay. (B) Sand. Positive values indicate that more sediment was transported into the channel reach than out of it, and therefore was accumulated within the reach. Note the difference in ordinate scales. Abbreviations as in Figure 3.

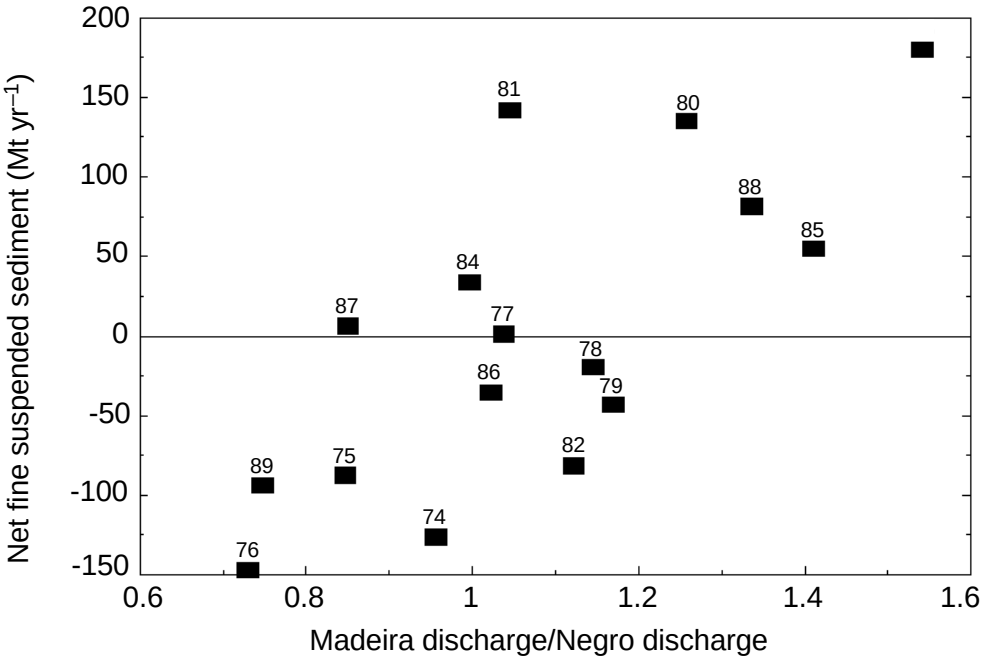

Figure 6. Relationship between the net transport of silt-clay through the Paurá-Óbidos reach and the ratio of annual flows from the Negro and Madeira Rivers (r^2 = 0.53; α < 0.001). The numerals indicate specific water years.

osition *(D_{bar})* were based on planimetric measurements of channel migration, surveys of bank heights, and particle-size analyses of flood-plain sediments. Rates of bank erosion and bar-island growth were measured as areas per unit length of the main channel from two maps covering a period of approximately 9 yr from 1971–1972 to 1980 (e.g., Mertes et al., 1996, Fig. 3). Rates measured over this short period of time were confirmed by qualitative analysis of historical maps and records dating back to the 1850s (Mertes et al., 1996, Figs. 9–11).

To translate a planimetric area to a volume of sediment added to or subtracted from the channel sediment load requires estimating the height of the area deposited or eroded. We assumed that each areal measurement represented an entire column of sediment from the surface to the channel bed. To calculate this height two values were estimated for each reach of the river. First, the low-water depth of the river was calculated from Brazilian Navy piloting charts. Second, the height of the bank above the low-water surface was measured in the field. For new bars and islands this above-water height averaged 2 m. The heights of older eroding banks, estimated from hand-level surveys at 20 sample points in the study reach, averaged 11 m in the upstream reaches, 10.5 m in the middle reaches, and 8 m in the downstream reaches (Mertes et al., 1996, Fig. 5).

The measurement technique for bar deposition accounts only for that sediment deposited within and adjacent to the channel. Sediment that is transported overbank and comes to rest on older flood-plain surfaces is evaluated in the next section. Volumes were converted to weight using a porosity of 0.35 and a particle density of 2600 kg m^{-3}. Grain-size composition of the near-bank flood-plain sediment was also measured at each sample site, and interpolated to estimate different sand-silt-clay distributions for each reach; overall averages through the entire study reach are 12-70-18 for eroded banks and 17-66-17 for freshly deposited bar sediments (Mertes, 1990, unpublished data).

Rates of bank erosion and bar deposition, are positively correlated, although bar-deposition rates are only about one-quarter of the bank-erosion rates. Sediment input per unit length of channel is weakly correlated with sinuosity (α < 0.10) measured by Mertes et al. (1996, Fig. 6), which varies with flood-plain width (α < 0.01). Thus, the relative degree of channel confinement imposed by the structural features appears to affect this component of the channel sediment budget. Bar deposition is complicated by midchannel deposition as well as by point-bar growth, and no simple relationship to sinuosity is apparent.

The rates of exchange of sediment with the flood-plain through channel shifting (Fig. 4) are remarkably high: 1570 Mt yr^{-1} are eroded from the flood plain (equivalent to 108% of the annual transport into the study reach and 127% of the flux past Óbidos), and 380 Mt yr^{-1} are deposited as bars (26% and 30%, respectively). The rates per unit length of channel (Fig. 4) follow the downstream pattern of channel migration (Mertes et al., 1996, Figs. 9–11), which is most rapid where the river is not confined by resistant terrace materials downstream of Santo Antônio do Içá, and bends that have relatively small radii of curvature are free to migrate. Farther downstream, bank erosion and bar deposition gradually diminish as the bends are larger and are partially constricted against the southern margin of the flood plain by neotectonic tilting (Tricart, 1977). Between Anorí and São José do Amatarí, migration is less where the river crosses the Purús arch, and it is greater where the river is unconfined downstream of the River Madeira confluence.

Diffuse Overbank Deposition

Deposition *(D_{ovrbk})* onto old flood-plain and bar surfaces (i.e., surfaces that do not appear as new bar deposition between 1971 and 1980) was calculated as the overbank flux of water in each reach multiplied by the sediment concentration of the near-surface water being decanted from the main channel and by the trap efficiency of the flood plain. Overbank flow rates were calculated from the Muskingum flood routing previously re-

ferred to. Once the volume of water in the channel had filled to the bankfull capacity:

$$\left(q_u - q_d\right)\Delta t = \Delta h \Delta x\left(w_c + 2w_f\right), \quad (2)$$

where q_u and q_d are, respectively, the water discharges at the upstream and downstream ends of a reach; Δt is the time step of the calculation; Δh is the change in water depth above bankfull stage; Δx is the length of the reach; w_c is the bankfull channel width; and w_f is the width of the flood-plain zone on each side of the channel that is inundated with water emerging from the channel. The value of w_f was measured from the width of flood-plain water observed on Landsat images to be colored with sediment-rich Andean water (Mertes, 1997). Since w_f changed very slowly through the flood season, we assumed it to be constant and used it to calculate the fraction of the water accumulating in the reach that flowed into the flood plain. This proportion entering the flood plain $[2w_f/(w_c + 2w_f)]$ was about 80% upstream of Jutica and 90% downstream of that station. The remaining portion increased the depth of water in the channel.

The role of levee breaks and flood-plain channels in conveying water into the flood plain below bankfull stage was not included in the flood routing, and is considered in the next section. These approximations and the 10%–20% error in the routed Muskingum flows (Richey et al., 1989b) degrade our estimate of the rates of overbank flow. Calculated average overbank discharges of water range from 0.04 m^3s^{-1} per meter of bank (maximum of 0.09) in the Santo Antônio do Içá–Xibeco reach to 0.4 m^3s^{-1} (maximum 0.7) for the Paurá-Óbidos reach. For the Manacapurú reach, in which Mertes (1994, p. 173) measured in the field and computed with a two-dimensional numerical simulation overbank discharges of 0.4–0.6 m^3s^{-1}, our method gives an average of 0.2 m^3s^{-1} and a daily maximum of 0.35 m^3s^{-1} per meter of bank.

We estimated the sediment concentrations of the surface water as a fraction of vertically averaged concentrations, based on a few simultaneous measurements of both values (Meade, 1985, Table 3; Mertes, 1994; Mertes et al., 1993; Mertes, unpublished samples). We estimated the ratio, which should vary with water-surface gradient, flow depth, and particle size (Vanoni, 1975; Aalto, 1995), to be about 0.33. Thus, vertically averaged sediment concentrations from our cruises at the season when water was flowing from the channel to the flood plain (December–May in the São Paulo de Olivença–Jutica reaches; February–May in the Jutica–São José do Amatarí reaches; and February–July in the São José do Amatarí–Óbidos reaches) were multiplied by 0.33 to estimate the surface sediment concentrations. Estimated values decreased gradually downstream from 140 mg l^{-1} at Vargem Grande to 80 mg l^{-1} at Óbidos because of dilution by tributary waters, the increasing water depth, and the generally diminishing gradient. Our surface samples contained too little material for textural analysis. Samples of sediment newly distributed across the flood-plain surface had sand concentrations of 2%–10% in the Manacapurú reach and less than 5% near Óbidos. Sand composed 25%–35% of samples collected from the edges of the banks (Mertes, 1990), where one would expect them to overrepresent the sand concentrations of the flow leaving the channel. Thus, for our calculation we used an average sand fraction of 10% for the channel-surface water entering the flood plain. This value probably overestimates the fraction in overbank flow in downstream reaches.

Calculated instantaneous rates of overbank sediment transport per meter of bank (Fig. 7) average 0.3–4.7 t day^{-1} m^{-1}. The high values in the Xibeco-Tupé-Jutica reaches may be slightly exaggerated due to errors in the flood routing. When the flow routed from Santo Antônio do Içá to Itapeua was compared with the measured record at the latter station, the predicted flow rose more slowly than the measured values. This rout-

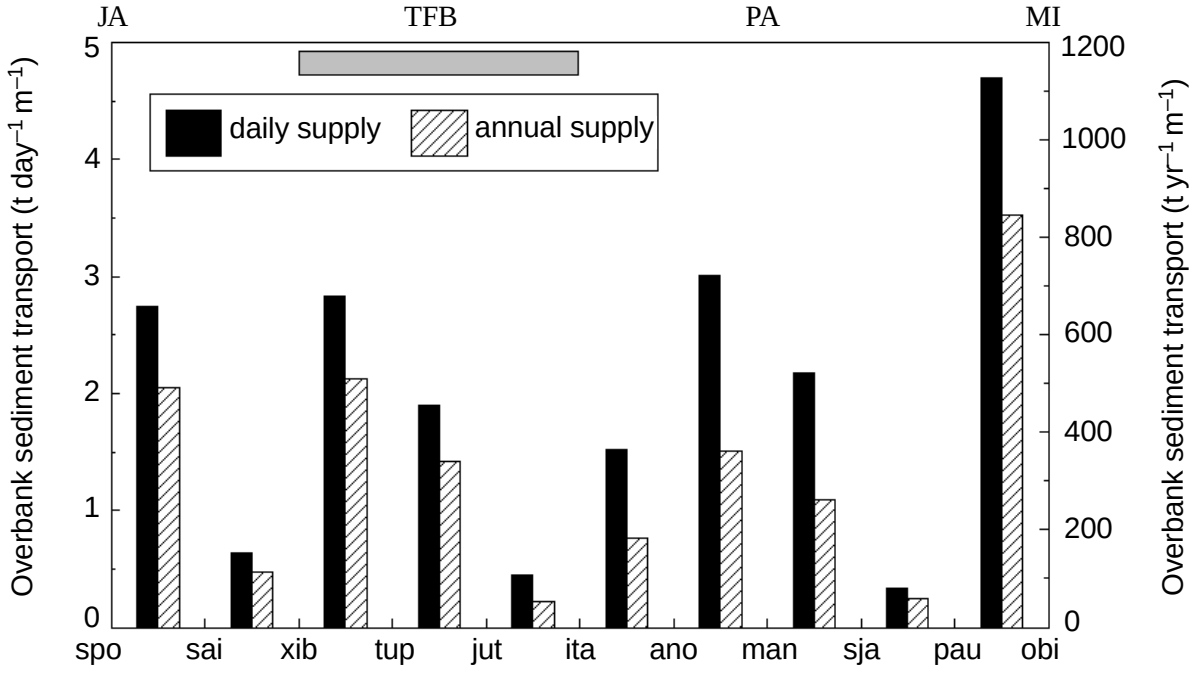

Figure 7. Computed rates of sediment transport in diffuse overbank flow. The left bar of each pair indicates the average daily rate of transport per meter over each bank during the season of overbank flow, calculated from flood routing of daily flows throughout 1974–1989. The right bar of each pair indicates the average annual overbank transport per meter. Abbreviations as in Figure 3.

ing error produced a progressive underestimation of in-channel flows past Tupé and Jutica and overestimation of the discharge of water, and therefore of sediment, into the flood plain. At Itapeua, the error was corrected by using the measured discharge when calculating the overbank flow, which would result in an underestimate of overbank fluxes in the Jutica-Itapeua reach. However, the maximum exaggeration of overbank flow was 6000 m^3s^{-1} into the 477-km-long Xibeco-Jutica reach. Assuming a linear increase in this error from zero at the beginning of rising water to 6000 m^3s^{-1} at the peak, approximately 200 days later, and a surface sediment concentration of 100 mg l^{-1} leads to an overestimate of about 10 Mt yr^{-1} out of 390 Mt yr^{-1} of overbank sediment transport in the Xibeco-Jutica reaches. The Jutica-Itapeua overbank flux, currently estimated to be 19 Mt yr^{-1}, is similarly underestimated by 10 Mt yr^{-1}.

Despite this error, the calculated pattern of high overbank sediment flux between Xibeco (rkm 1051) and Jutica (rkm 1528) and low flux between Jutica and Itapeua (rkm 1704) is consistent with the presence of a wide flood plain and low bank height in the former reach and a narrow flood plain with an abrupt increase in bank height in the Jutica-Itapeua reach (Mertes et al., 1996, Figs. 5 and 6). Similarly, overbank fluxes are low in the São José do Amatarí–Paurá reach (Mertes et al., 1996, cover photo of that journal), where a high terrace on the northern bank, well-developed scroll bars and levees on the southern bank (probably consisting of sediment from the nearby River Madeira), and the accumulation of large amounts of locally generated water confine the sediment-rich water to the main channel. Confidence that the results are approximately correct also arises because the calculated rates of sediment transport for the season of flow from the channel to the flood-plain average 3 t d^{-1} per meter of bank in the reach near Manacapurú; this is where Mertes (1994, p. 172) measured values averaging 3–5 t day^{-1} m^{-1} and calculated values of 4–18 t day^{-1} m^{-1} from remotely sensed surface concentrations and a two-dimensional hydrodynamic model of flow across the flood plain during two floods.

We did not sample diffuse flow draining from the flood plain to the channel, but our visual observations indicated that the flow was more or less devoid of sediment, except where it drained from flood-plain channels, probably because of aggregation of the silt-clay particles leaving the channel (Stallard and Martin, 1989; Nicholas and Walling, 1996). Mertes (1994) used remote sensing of surface sediment concentrations and hydrodynamic flow simulation to map sediment fluxes across a flood plain near Manacapurú, indicating that approximately 90% of the sediment leaving the channel was deposited within a few hundred meters of the levee. However, the relatively narrow zone of turbid water visible on Landsat images during the flood season indicates that this water does not spread far from the channel and reenters it after only a few kilometers of flow across the flood plain (Mertes, 1997). Average annual overbank deposition was thus calculated as 90% of the overbank flux for the period 1974–1989, and ranged from 60 t m^{-1} yr^{-1} on each side of the channel in the confined Jutica-Itapeua reach to 770 t m^{-1} yr^{-1} between Paurá and Óbidos. When summed over the entire study reach, this deposition amounts to 1105 Mt yr^{-1} of silt-clay (equivalent to 112% of the transport past Óbidos) and 124 Mt yr^{-1} of sand (equivalent to 50% of the Óbidos export). Values for individual reaches are plotted as the fourth bar of each set in Figure 4.

Channelized Overbank Deposition

We calculated the annual sediment load decanted from the channel into and trapped within flood-plain channels (Fig. 1) that leave and rejoin the main channel. The strategy involved multiplying the estimated water outflow from the main channel to the flood-plain channels by the mainstem sediment concentration, averaged over the depth range of the flood-plain channel, and by a trap efficiency for the flood-plain channel.

The water discharge into the flood-plain channel was calculated from Manning's formula:

$$q_{fpc} = \frac{a_{fpc} R^{0.67} s^{0.5}}{n}, \qquad (3)$$

where q_{fpc}, a_{fpc}, R, s, and n are, respectively, the water discharge, cross-sectional area, hydraulic radius, gradient, and hydraulic roughness of each flood-plain channel in SI units. We measured the widths and low-water depths of all 105 flood-plain channels in the 2010 km reach between São Paulo de Olivença and Óbidos mapped on the 1:100 000 scale Brazilian Navy piloting charts (Mertes et al., 1996, Fig. 13). Since the deposition of sediment spreads from the upstream ends of the flood-plain channels, the depths were measured over tabular sills 0.5–5 km long with the assumption that these features control the flow entering the flood-plain channel for a given water-surface elevation in the main channel. Addition of the stage change between low water and any other mainstem discharge allowed us to compute the associated flow depths in the flood-plain channels. Low-water flow depths ranged to 16 m, high-water depths to 30 m, and widths to 2000 m. During the period of rising water, there is little flow from the flood plain into the flood-plain channels. The assumption of steady uniform flow, implicit in the Manning equation, does not extend to the entire length of the flood-plain channel because of the increase in flow depth beyond the tabular sill, but this is not likely to cause errors that are significant for the present purpose.

Using regression on cross-section surveys of five flood-plain channels of widely differing sizes (data reported by Mertes, 1990), we estimated a_{fpc} as 0.8 times the width-depth product, and R as 0.8 times the flow depth. We measured the ratio (which varied from 0.8 to 2.0) between each flood-plain channel length and the associated main channel length, and used this ratio to calculate the flood-plain channel gradient from the mainstem water-surface gradient at various flows. (See the discussion of the seasonal variation of water-surface gradients in the earlier section on channel gradient.) Manning's roughness coefficient was assumed to be 0.03 for sand-bed channels (Henderson, 1966, p. 99).

The sediment concentrations of water decanted into flood-plain channels were estimated as for the diffuse overbank flow, except that the surface sediment concentrations in the main channel were increased by 1.25 for silt-clay and by 2.0 for sand, reflecting the vertical distribution of the two textural classes averaged over typical depth ranges of flood-plain channels (Aalto, 1995). The result of this generalization was that 85% of the computed sediment export to the channels was silt-clay and 15% was sand.

We calculated sediment fluxes into flood-plain channels for the highest recorded stage in the main channel and for an early-rising stage, 4 m above low water, to bracket the range of conditions between high water–low sediment concentration and low discharge–high sediment concentration. The computed flow velocities in flood-plain channels decreased irregularly downstream as gradient diminished, and averaged 1.2 m s^{-1} at high flow with a range from 0.5 to 2.3 m s^{-1}; they averaged 0.75 (0.25–1.6) m s^{-1} at early-rising water. There was an irregular downstream increase in the largest flood-plain channel discharge in a reach as the decrease in velocity was offset by the increase in the widths of the larger flood-plain channels. The discharges for the 105 flood-plain channels were exponentially distributed; the high-water mean was approximately 8800 m^3 s^{-1} (range 700–41 000) and the early-rising mean was 4050 m^3 s^{-1}(0–25 000). The flood-plain channels thus approach diffuse overbank flow at one end of the distribution and major anabranches of the Amazon at the other.

The downstream decrease in sediment concentration and the irregular increase in flood-plain channel discharge combined to yield no alongstream trend in channelized sediment export from the main stem (Fig. 8A). Sediment fluxes into flood-plain channels ranged from

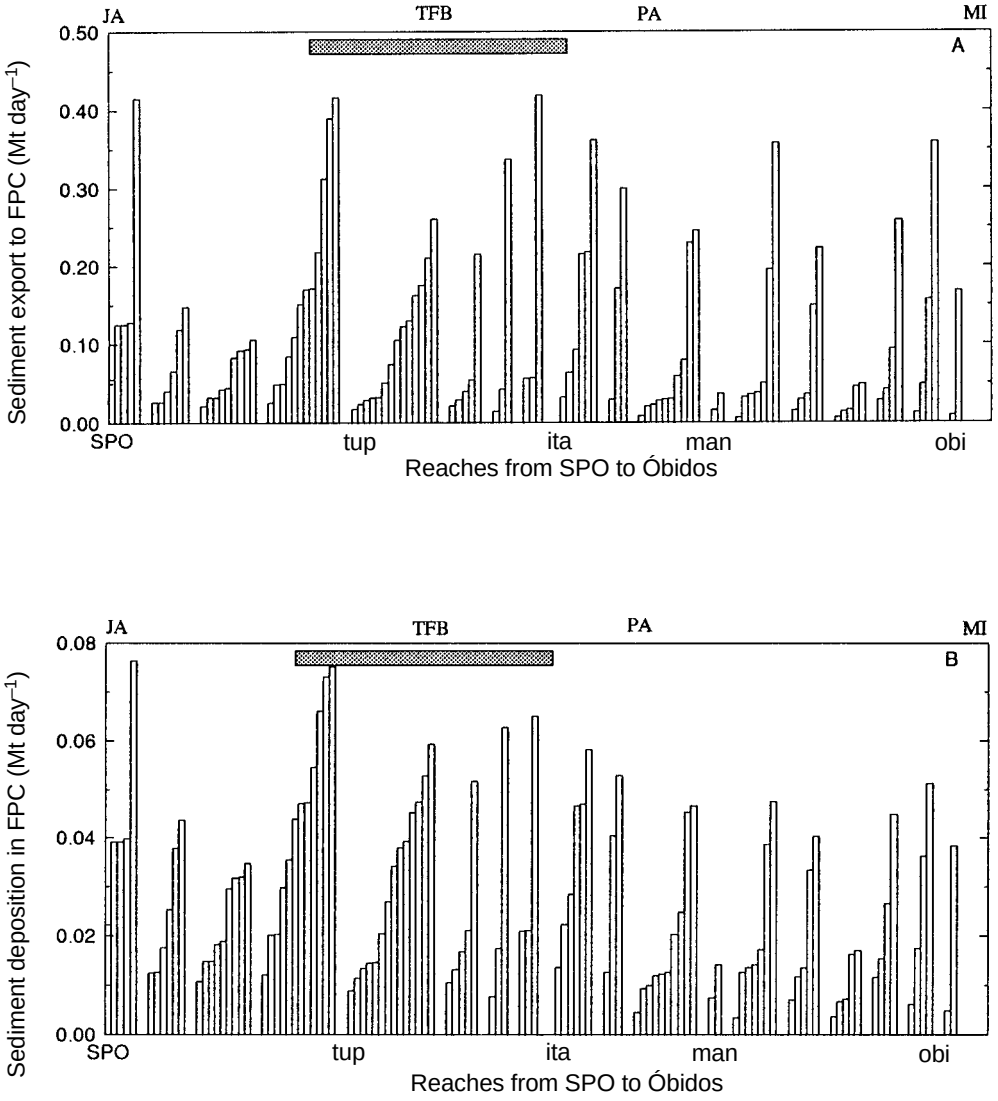

Figure 8. Computed daily rates of (A) sediment export into and (B) deposition within each of the 105 flood-plain channels at peak flow. Note the difference in ordinate scales. The bars indicate each value within a sampling reach and do not imply downstream increases within each reach. Abbreviations as in Figure 3.

0.002 to 0.34 Mt day^{-1} (mean = 0.07 Mt day^{-1}; median = 0.025 Mt day^{-1}) for early-rising water and from 0.007 to 0.42 Mt day^{-1} (mean = 0.11 Mt day^{-1}; median = 0.06 Mt day^{-1}) at peak flow. The small range between the two time periods was due to the offsetting effects of increasing water discharge and decreasing sediment concentration on the rising limb of the hydrograph.

We hypothesized that trap efficiencies of flood-plain channels would scale inversely with discharge because the greater depths and velocities of flows in the larger channels favored keeping sediment in suspension. Using measured sediment inflows and outflows of 5 flood-plain channels having discharges ranging from 23 to 5600 m^3 s^{-1}(Mertes, 1990), we regressed trap efficiency against the logarithm of discharge. The resulting inverse relationship (trap efficiency [percent] = 128 – 10.8 ln q_{fpc}), although significant at the 0.05 level, has a poorly defined slope. The relationship was used only as a rough guide of how trap efficiencies range from 95% to 100% for the smallest flood-plain channels (~10–20 m^3 s^{-1}) to approximately 10% for the largest (~50 000 m^3 s^{-1}), thus merging with the behavior of diffuse overbank flow at the smaller end of channel sizes and with major anabranches of the Amazon mainstem at the other. With a larger sample of channels, we might have been able to improve the estimation of trap efficiency by including gradient in the analysis, but this did not reduce uncertainty with the current data set.

We then multiplied the export rate of sediment into each flood-plain channel by its trap efficiency, estimated from its discharge, to calculate the sedimentation rates at early-rising and high flows (Fig. 8B). These deposition rates averaged 0.02 Mt day^{-1} (maximum 0.07) for rising water, and averaged 0.03 Mt day^{-1} (maximum 0.08) for the peak. The deposition rate diminished gradually downstream because of the declining trap efficiencies associated with larger flood-plain channel discharges. In the downstream reaches, more flood-plain channels behave like anabranches of the main channel; sediment is swept through them and back into the channel. To compute the contribution of flood-plain channel sedimentation in each reach, we averaged the high and low values of deposition for each flood-plain channel and multiplied by the annual number of days of flow into the flood-plain channel (120 between Jutica and São José do Amatarí; 180 days upstream and downstream) and summed the results by reach (Fig. 9).

Upstream of the confined reach that begins at Jutica, flood-plain channel deposition is in the range 0.29–0.33 Mt yr^{-1} km^{-1}. In the Jutica–São

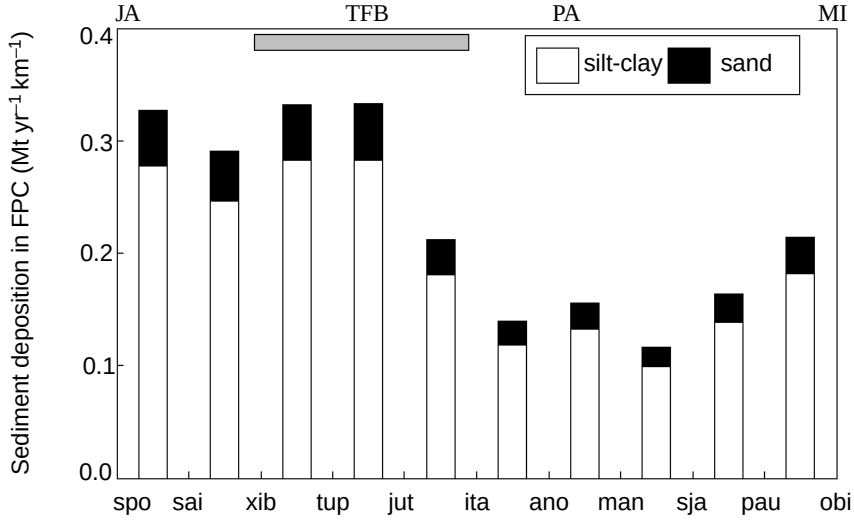

Figure 9. Annual rates of sedimentation in all flood-plain channels in each reach. Abbreviations as in Figure 3.

José do Amatarí reach there are fewer flood-plain channels and a shorter duration of overbank flooding in the narrower flood plain, and flood-plain channel sedimentation begins to decline, reaching a minimum of 0.12 Mt yr^{-1} km^{-1} in the Manacapurú–São José do Amatarí reach. Downstream of the Purús arch and the River Madeira mouth, where the flood plain begins to widen again (Fig. 3), mainstem sediment concentrations are low and the flood-plain channels are so large and their trap efficiencies so low that the deposition rate does not rise to upstream values, despite the increased duration of flow into the flood-plain channels. Flood-plain channel sedimentation varies from 0.33 to 2.0 times the diffuse overbank sedimentation upstream of the Purús arch, but downstream the fraction lies in the range 0.10–0.23, except near the mouth of the River Madeira,where both forms of sedimentation are suppressed (Mertes et al., 1996, cover photo).

Mainstem Channel Storage

The final term in the mass balance of equation 1 is defined as the annual rate of change in channel storage, including sediment eroded from or deposited on the channel bed or between the landward edge of a bar (2 m above average low-water stage) and the main channel bank. Accumulation of sediment in the channel would plot in the positive field in Figure 4. However, since it is derived only as a residual, the same term also includes any overlooked sediment transport processes or errors of estimation. For example, sediment eroded from a bank (such as a terrace) higher than 8–11 m above the low-water stage mapped on navigation charts would be underestimated, and the error would tend to indicate scour or lower accumulation in Figure 4. Uncertainties in sediment-rating curves, and in measured or computed flow records, may have led to positive and negative residual errors. Another potential source of error is the disparity in time between the data used to estimate each sediment flux in equation 1. A second set of potential problems is the difficulty of measuring some of the quantities used, as we have emphasized herein. For example, we described earlier how bias in the flood-routing scheme for computing overbank sediment flux probably caused an error in that sediment-budget term between Xibeco and Itapeua. However, the errors are confined within those reaches. We have not been able to devise a scheme for quantification of all conceivable errors in the various estimation techniques.

Because of our concern about errors accumulating in the residual term, we highlighted the storage term in Figure 4 by using squares linked by lines, rather than bars. The question of error is particularly important because the term is a large fraction of the sediment balance of most reaches. It is important, therefore, to know whether the alongstream pattern of these residuals is dominated by errors or reflects real channel-storage processes. Confidence in the latter case arises from: (1) the interannual consistency of the net suspended-sediment transport quantities (Fig. 5); (2) the roughly correlated behavior of the two textural classes (which is partly but not wholly due to the assignment of fixed proportions of sand and silt-clay in the computation of E_{bk}, D_{bar}, D_{ovrbk}, and D_{fpc}); and (3) the fact that the other quantities in equation 1 are explainable in terms of hypothesized controlling factors, as demonstrated in foregoing sections. Viewed in this light, the storage term also behaves in a reasonable manner.

Although the individual channel-storage changes are probably within the limits of resolution of our techniques for most reaches, we include the results from all reaches in the following discussion since they suggest trends that may be investigated through further monitoring. The patterns of sediment removal or accumulation are associated with changes in gradient and discharge along the river, and therefore, apparently, with changes in the long-term sediment-transport capacity of each reach. Figure 4A demonstrates that the silt-clay storage is negative (implying net channel erosion) from São Paulo de Olivença to Jutica, from Anorí to São José do Amatarí, and from Paurá to Óbidos. Sand storage is also negative upstream of Jutica and in the Paurá-Óbidos reach (Fig. 4B). Despite the fact that the sampling stations do not exactly match the breaks in gradient indicated by the satellite altimetry in Figure 3, in each of these eroding reaches (rkm 740–1528, rkm 1885–2228, and rkm 2474–2750) the channel gradient increases downstream as the river crosses structural features and the channel is confined. The downstream steepening increases the sediment-transport capacity of the river beyond the increment of sediment supplied to the channel in these reaches. The Anorí–São José do Amatarí (rkm 1885–2228) reach also receives a large increment of sediment-free water from the River Negro. The Paurá-Óbidos reach receives water from the River Madeira, along with a sediment load that is larger than the influx to São Paulo de Olivença, but the net effect is still for sediment to be scoured from the steepening reach. Where channel gradient decreases downstream, between Jutica and Anorí (rkm 1528–1885) and

between São José do Amatarí and Paurá (Rkm 2228–2474), silt-clay is deposited along the channel (positive values in Fig. 4A). Sand accumulates in the channel throughout the reach downstream of Jutica, but there is a strong minimum in Manacapurú–São José do Amatarí reach (rkm 2031–2228) because of the flushing action of the Negro River outflow.

The association between downstream changes of gradient and changes in channel storage is strengthened by a calculation that can be made for the reach downstream of Óbidos, where the channel gradient appears to be declining slightly on the downstream side of the Monte Alegre intrusion (Fig. 3). Mertes and Dunne (1988) estimated that an average of 300–400 Mt of sediment (0.67–0.89 Mt yr^{-1} km^{-1}) are deposited each year in the 450 km reach between Óbidos and the coast, where the river divides into several distributary channels before entering the coastal zone. They based this conclusion on the difference between the estimated sediment discharge at Óbidos (then estimated to be 1100–1300 Mt yr^{-1}) and the sum of deposition on the continental shelf (610–650 Mt yr^{-1}; Kuehl et al., 1986) and the rate of along-shelf sediment transport (100–200 Mt yr^{-1}, estimated by Augustinus, 1982; Nittrouer et al., 1986). The budget was essentially confirmed by Nittrouer et al. (1995). We hypothesize that most of this sediment is deposited between the Monte Alegre intrusion and the Gurupá arch (approximately rkm 2800–3200 in Fig. 3B). Radar imagery there (Radambrasil, 1972) reveals a sudden change in the alluvial morphology (Mertes et al., 1996, Fig. 16, c and d), from a flood plain occupied by hundreds of lakes to a delta plain that appears to have been filled as the average water-surface gradient decreases essentially at sea level, but where the water is still fresh.

The rates of sediment removal and accumulation for reaches implied by the storage term in Figure 4 range to 16 cm yr^{-1}, except in the São Paulo de Olivença–Santo Antônio do Içá reach. The calculated scour of 40 cm yr^{-1} there is almost certainly an error in estimating small differences between inputs and outputs in the vicinity of the River Içá confluence. In particular, if the calculated storage changes are even approximately correct, they imply channel lowering of 0–3 cm yr^{-1} in the São Paulo de Olivença–Jutica reach and 5–6 cm yr^{-1} in the Manacapurú reach. Downstream of Jutica, they indicate the channel bed to be rising at approximately 2–4 cm yr^{-1} during the period of our measurements. Downstream of the mouth of the River Madeira, calculations predict the bed to be rising at 16 cm yr^{-1}, and upstream of the Monte Alegre high to be lowering at 12 cm yr^{-1}. Records of channel-bed elevation at gauging stations are not long enough to indicate whether the implied changes have taken place.

The storage portrayed in Figure 4 refers to annual totals. There are seasonal patterns of net flux, such as the one documented for the Manacapurú-Óbidos reach by Meade et al. (1985), and interpreted to be due to settling and resuspension of sediment resulting from changes in water-surface gradient caused by the timing of water inflows from the major tributaries. A more comprehensive analysis of the same seasonal variations in net flux confirms that silt-clay accumulates in all the reaches between Manacapurú and Óbidos during early to mid-rising water and then is removed at higher and later stages. The deposition of sand persists a little later into the flood season and is reestablished sooner on the declining hydrograph. However, the bed-material samples from Amazon cruises (Mertes and Meade, 1985, Table 2) indicate that the silt-clay "disappearing" from the flux measurements is not settling to the bed, although it may be draping the banks and levees. Even at early-rising water, it is rare to find bed material containing more than a few percent silt-clay in the main channel. This finding suggests that the seasonal dynamics of silt-clay transport are modulated through exchanges with the channel margins or flood plain rather than simply by in-channel settling and resuspension. The other analyses in this paper indicate that the sediment budgets of Amazon reaches are subject to exchanges with the flood plain that dwarf the seasonal differences in net suspended flux, even though we cannot yet resolve them at a subannual scale.

CHANNEL–FLOOD-PLAIN SEDIMENT BUDGET

Figures 4 and 10 summarize the sediment budget of each channel reach along the entire 2010 km of the Amazon River between São Paulo de Olivença and Óbidos for the period of our estimate. The preceding text also describes a less-detailed estimate of deposition rate in the delta plain downstream of the Monte Alegre intrusion, for a combined reach length of 2460 km. Tables 2 and 3 indicate that an average of 616 ± 44 Mt yr^{-1} of sediment entered the channel at the upper end of the study reach (São Paulo de Olivença) and were augmented by 117 ± 8 Mt yr^{-1} from the lowland tributaries and 715 ± 94 Mt yr^{-1} from the River Madeira, despite the long passage of this tributary across the Brazilian craton. The annual sediment flux past Óbidos averaged 1239 ± 130 Mt yr^{-1}, indicating an average annual accumulation rate in the reach of approximately 209 Mt yr^{-1} (14% of the influx); the standard error of the storage term was 167 Mt yr^{-1} (Table 3). The calculated silt-clay storage was 151 Mt yr^{-1} (14% of the input), which was less than its standard error (161 Mt yr^{-1}); for sand the calculated storage was 58 Mt yr^{-1} (19% of the input), and the standard error 44 Mt yr^{-1}.

Exchanges between the channel and flood plain in each direction exceeded the annual channelized sediment transport into or out of the reach (Table 3). The annual supply of sediment entering the channel from bank erosion was computed to be 1570 Mt yr^{-1}. An estimated 380 Mt yr^{-1} were transferred to bar storage, while 1690 Mt yr^{-1} were transferred to the flood plain (460 Mt yr^{-1} in channelized flow; 1230 Mt yr^{-1} in diffuse overbank flow). Calculated deposition on the bars and flood plain exceeded bank erosion by 500 Mt yr^{-1} (32% of the bank erosion supply). Thus, we have two independent estimates of net sediment accumulation in the 2010 km reach: approximately 200 Mt yr^{-1} and 500 Mt yr^{-1}, which agree in sign and general magnitude, thereby crudely validating our attempts to calculate individual channel–flood-plain exchanges. Of the remaining flux past Óbidos, another 300–400 Mt yr^{-1} (24%–32%) do not reach the ocean, but are deposited in the delta plain.

The sediment budget of the 2010 km reach indicates that transport of material through the valley is strongly modulated by exchanges of sediment with the flood plain, annual values of which exceed the channel transport. Exchanges with the flood plain involve both hydrological processes such as overbank flooding and export to flood-plain channels, and morphological changes such as bank erosion and bar deposition (Figs. 1 and 4). When compared to the annual channel sediment transport, using the average flux past Óbidos (1240 Mt yr^{-1}) as a scale equal to 1.0, the other terms in the sediment budget for the valley have magnitudes of: São Paulo de Olivença influx = 0.5; Madeira influx = 0.6; other tributaries = 0.1; bank erosion = 1.3; bar deposition = 0.3; diffuse overbank deposition = 1.0; deposition in flood-plain channels = 0.4.

If the relative magnitudes of the sediment exchanges are typical of other rivers that have large flood-plains, there are important implications for the transport and storage of hydrophobic materials associated with sediments. For example, Figure 10 illustrates that between São Paulo de Olivença and São José do Amatarí the channel transport remains fairly constant at 600–700 Mt yr^{-1}. Between the two sections, bank erosion contributes a total of about 1300–1400 Mt yr^{-1}, and deposition on the bars and flood plain removes an equal or larger amount. It is reasonable to expect, therefore, that all or most of the sediment passing Óbidos has spent time in the flood plain during transit through the valley, and that most of the sediment passing São Paulo de Olivença in 1 yr might be entirely deposited before reaching São José do Amatarí.

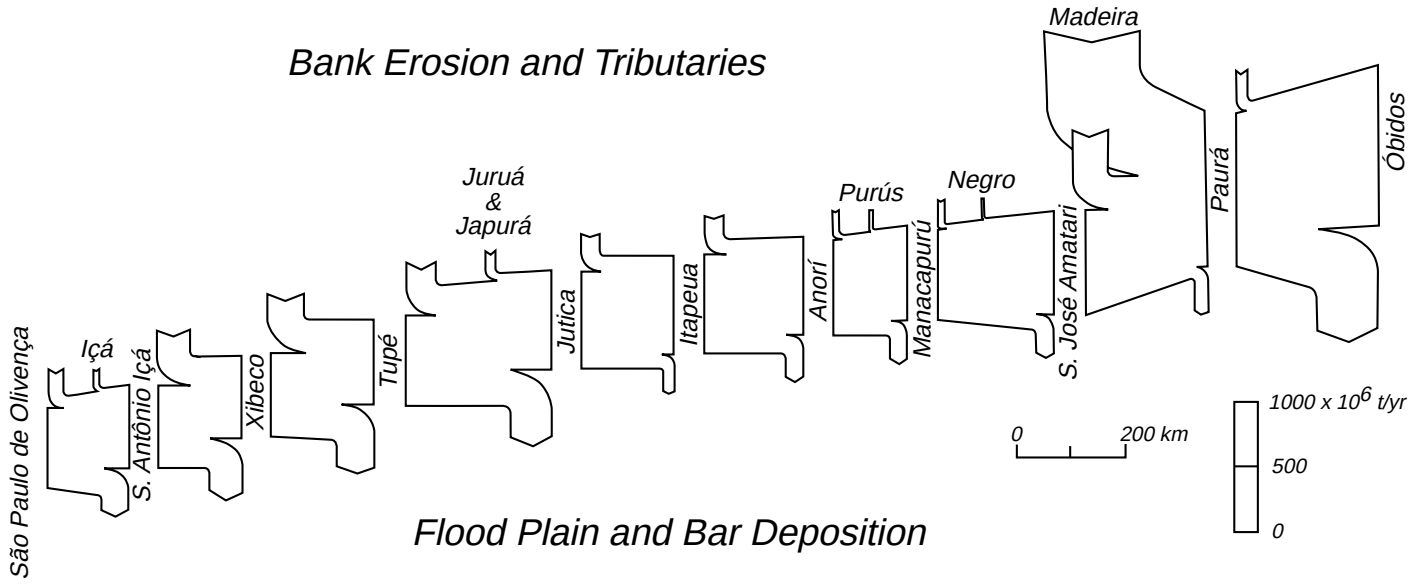

Figure 10. Sediment budget for the 2010 km reach of the Amazon River between São Paulo de Olivença and Óbidos, Brazil, summarizing the budgets measured and calculated for each of the 10 reaches (ranging in length from 146 to 280 km) between river cross sections where enough sediment-discharge values have been measured to generate a sediment rating curve, and thus to compute a long-term sediment flux. The diagram has been exploded at each measurement section so that the individual budgets for each reach may be inspected. Represented in the upper left corner of the plot for each reach is the bank erosion. Represented in the lower right of each plot is the deposition on bars and flood plains (both overbank and in channels). Tributary inputs are shown along the upper parts of the plots; especially prominent is the large input of sediment from the Madeira River.

TABLE 3. SUMMARY OF THE CHANNEL–FLOOD-PLAIN SEDIMENT BUDGET FOR THE REACH OF THE AMAZON RIVER VALLEY BETWEEN SÃO PAULO DE OLIVENÇA AND ÓBIDOS, BRAZIL

Channel sediment transport		
Input from São Paulo de Olivença	616	(±44)
Input from lowland tributaries	117	(±8)
Input from River Madeira	715	(±94)
Output at Óbidos	1239	(±130)
Accumulation in reach	209	(±167)
Channel-flood plain exchange processes		
Bank erosion	1570	
Bar deposition	380	
Diffuse overbank sedimentation	1230	
Channelized flood plain sedimentation	460	
Net transfer to flood plain	500	

Notes: Values are in Mt yr^{-1}. Numbers in parentheses are standard errors of the estimated means for the calculations based on sediment sampling in channels. Another 300–400 Mt yr^{-1} are deposited in the delta plain downstream of Óbidos.

Alongstream patterns in each of the terms of the decadal sediment budget (see Fig. 4 and its discussion) are associated with features apparently produced by intracratonic tectonics and major tributary inputs of water and sediment. Some of the storage changes are within their standard errors and are included only as working hypotheses, while the uncertainities are reduced by further sediment sampling. The following patterns, however, are remarkably consistent. The river is confined by cohesive terraces as it crosses the Purús arch and the Monte Alegre high, and thus the flood plain narrows. At the downstream end of the fault block, the river is also diverted against the southern terrace by tilting of the valley floor toward the south-southeast. In these reaches, the river's sinuosity and migration rate are decreased and the gradient increased. The resulting downstream sequence of increasing and then decreasing gradient (Fig. 3) is associated, respectively, with scour and then with accumulation within the channel (square symbols in Fig. 4), the pattern being complicated slightly by scour of silt-clay downstream of the sediment-poor River Negro. In the reaches from São Paulo de Olivença to Jutica, the gradient generally increases (Fig. 3B) and the squares in Figure 4 indicate scour. Low gradients between Jutica and Anorí are associated with net accumulation. The increase in gradient as the Purús arch is approached leads to scour of silt-clay and a reduction in the accumulation of sand. Downstream of the arch, the gradient decreases, but the massive inflow of sediment-poor water from the River Negro causes scour of silt-clay and a reduction (to zero) in the accumulation of sand. Low gradient downstream of São José do Amatarí and the large sediment supply from the River Madeira cause deposition of both textural classes in the next reach downstream. The increasing gradient between Paurá and Óbidos is associated with net scour of both textures even as the river approaches tidewater. Downstream of the Monte Alegre intrusion, there appears to be a slight decrease in gradient, and in this reach rapid sedimentation occurs in the delta plain, as described in the section on mainstem channel storage.

The effect of gradient, however, is not simply to determine the suspended-load transport capacity of the channel, which is currently unknown. Instead, the tectonic activity (whether current or not) affects the form and behavior of the channel and flood plain (Fig. 3; Mertes et al., 1996), which together with the hydrology of the valley

floor controls the processes of bank erosion, bar deposition, and dispersion of sediment into the flood plain, as described herein.

CONTROLS ON SEDIMENT EXCHANGE BETWEEN CHANNEL AND FLOOD PLAIN

In this study we identified four major flood-plain–channel exchanges of sediment for a large, naturally functioning river. Their relative importance elsewhere will vary with the geomorphology, hydroclimatology, and management of particular rivers. We described the geomorphic and hydrologic processes that control the exchanges and channelized transport, and illustrated how they might be analyzed and predicted in other river valleys.

Several general principles are suggested by our analysis.

1. The bank and bar exchanges involve channel shifting, and at least the bank erosion is weakly correlated with channel sinuosity, and thus indirectly with flood-plain width. These exchanges can be evaluated for each grain size by multiplying together: average bank or bar height (as appropriate), grain-size composition, and the area of flood plain eroded or deposited in a period of time. Bank and bar elevations and textures are currently obtainable only through field surveys. Areas of erosion and deposition may be obtained by mapping channel changes, as done here, and projecting average rates into the future, or from calibrated predictions of channel migration, using an approach such as the bend theory of Ikeda et al. (1981) and Parker et al. (1982). In rivers that are rapidly depositing bed material because of alongstream changes in gradient and sediment transport capacity, channel shifting may also reflect these processes (Dunne, 1988, Fig. 7).

2. Diffuse overbank sediment transport is equal to the overbank flux of water (here calculated by flood routing) multiplied by the surface sediment concentration in the main channel and by the trap efficiency of the flood plain. It is therefore controlled by: (1) the average bank height; (2) the flood-conveyance hydrology of the main channel, including the pattern of water inflows, channel capacity, duration of overbank flooding, and the degree to which the spreading of turbid water into the flood plain is resisted by water accumulating there due to rainfall and local runoff (Mertes, 1997); (3) the surface sediment concentration in the main channel, which depends on texture, gradient, and flow depth; and (4) the hydraulic roughness of the flood plain, which affects the residence time of water on the flood plain and therefore the time available for settling.

3. The dispersion of sediment through flood-plain channels is equal to the water flow into each channel (calculated from flood-plain channel geometry and main-channel water stage) multiplied by the sediment concentration of main-channel water averaged over the depth of the flood-plain channel and by the trap efficiency of each flood-plain channel. This channelized deposition therefore depends on (1) the near-surface sediment concentration in the main channel (referred to above); (2) the duration of flow into each flood-plain channel; (3) the dimensions of the flood-plain channel; (4) its trap efficiency, which correlates with its discharge and possibly its gradient; and (5) the distribution of these flood-plain channel characteristics along the valley.

These principles should apply to all large channel–flood-plain systems and could be used as a basis for analyzing valley-floor sediment budgets and predicting their response to environmental and anthropogenic change.

ACKNOWLEDGMENTS

This work was supported by National Science Foundation grant BSR-8107522 for the CAMREX (Carbon in the Amazon River: An Experiment) Project, and National Aeronautic and Space Association–EOS (Earth Observing System) Amazon Project NAGW-2652 and NAGW-5233. The river discharge records were provided by E. Oliveira and V. Guimares of the Departamento Nacional de Agua e Energia Elétrica, Brasilia. We thank Dr. M. V. Caputo of Petrobras for advice on the tectonics of Amazônia, the Instituto Nacional de Pesquisas da Amazônia, Manaus for assistance in staging field work, R. E. Aalto, J. W. Kirchner, L. A. Martinelli, and T. Pimental, who assisted us at various stages of the field work and analysis, and B. Gomez, J. B. Ritter, and an anonymous reviewer for improving the manuscript. CAMREX contribution no. 87.

REFERENCES CITED

Aalto, R. E., 1995, Discordance between suspended sediment diffusion theory and observed sediment concentration profiles in rivers [Master's thesis]: Seattle, University of Washington, 97p.

Augustinus, P. G. E. F., 1982, Coastal changes in Surniname since 1948, *in* Proceedings of the Congress on the Future of Roads and Rivers in Suriname and Neighboring Region, Dec., 1982: Paramaribo, Suriname, Delft University of Technology, p. 329–338.

Bevington, P. R., 1969, Data reduction and error analysis for the physical sciences: New York, McGraw-Hill, 336 p.

Caputo, M. V., 1984, Stratigraphy, tectonics, paleoclimatology, and paleogeography of northern basins of Brazil [Ph.D. dissert.]: Santa Barbara, University of California, 583 p.

Caputo, M. V., 1991, Solimões megashear: Intraplate tectonics in northwestern Brazil: Geology, v. 19, p. 246–249.

Dietrich, W. E., 1982, Flow, boundary shear stress, and sediment transport in a river meander [Ph.D. dissert.]: Seattle, University of Washington, 261 p.

Dietrich, W. E., Dunne, T., Humphrey, N. F., and Reid, L. M., 1982, Construction of sediment budgets for drainage basins: Sediment budgets and routing in forested drainage basins: U.S. Forest Service General Technical Report PNW-141, Pacific Northwest Forest and Range Experiment Station, p. 5–23.

Dunne, T., 1988, Geomorphological contributions to flood control planning, *in* Baker, V. R., Kochel, R. C., and Patton, P. C., eds., Flood geomorphology: Chichester, United Kingdom, Wiley and Sons, p. 421–438.

Gibbs, R. J., 1967, The geochemistry of the Amazon River system: Part I. The factors that control the salinity and the composition and concentration of the suspended solids: Geological Society of America Bulletin, v. 78, p. 1203–1232.

Gomez, B., Mertes, L. A. K., Phillips, J. D., Magilligan, F. J., and James, L. A., 1995, Sediment characteristics of an extreme flood: 1993 upper Mississippi River valley: Geology, v. 23, p. 963–966.

Graf, W. L., 1994, Plutonium in the Rio Grande: Environmental change and contamination in the nuclear age: New York, Oxford University Press, 329 p.

Guyot, J. L., 1993, Hydrochimie des fleuves de l'Amazonie bolivienne [Etudes et Thèses]: Paris, Editions de l'ORSTOM, 261 p.

Guzkowska, M. A. J., Rapley, C. G., Ridley, J. K., Cudlip, W., Birkett, C. M., and Scott, R. F., 1990, Developments in inland water and land altimetry: University College of London, Mullard Space Science Laboratory, European Space Agency final contract report 7839/88/F/Fl, 26 p.

Henderson, F. M., 1966, Open channel flow: New York, Macmillan, 522 p.

Ikeda, S., Parker, G., and Sawai, K., 1981, Bend theory of river meanders, part 1: Linear development: Journal of Fluid Mechanics, v. 112, p. 363–377.

Jacobson, R. B., and Oberg, K. A., 1997, Geomorphic changes of the Mississippi River floodplain at Miller City, Illinois, as a result of the floods of 1993: U.S. Geological Survey Circular 1120-J, 23 p.

Johnsson, M. J., and Meade, R. H., 1990, Chemical weathering of fluvial sediments during alluvial storage: The Macuapanim Island point bar, Solimões River, Brazil: Journal of Sedimentary Petrology, v. 60, p. 827–842.

Kelsey, H. A., Lamberson, R., and Madej, M. A., 1987, Stochastic model for the long-term transport of stored sediment in a river channel: Water Resources Research, v. 23, p. 1738–1750.

Kesel, R. H., Yodis, E. G., and McCraw, D. J., 1992, An approximation of the sediment budget of the lower Mississippi River prior to major human modification: Earth Surface Processes and Landforms, v. 17, p. 711–722.

Knox, J. C., 1987, Historical valley floor sedimentation in the Upper Mississippi Valley: Association of American Geographers Annals, v. 77, p. 224–244.

Kuehl, S. A., DeMaster, D. J., and Nittrouer, C. A., 1986, Nature of sediment accumulation on the continental shelf: Continental Shelf Research, v. 6, p. 209–225.

Leenaers, H., and Rang, M. C., 1989, Metal dispersal in the fluvial system of the River Geul: The role of discharge, distance to the source, and floodplain geometry, *in* Sediment and the environment: International Association of Hydrological Sciences Publication 184, p. 47–55.

Leenaers, H., and Schouten, C. J., 1989, Soil erosion and floodplain soil pollution: Related problems in the context of a river basin, *in* Sediment and the environment: International Association of Hydrological Sciences Publication 184, p. 75–83.

Lewin, J., Davies, B. E., and Wolfenden, P. J., 1977, Interactions between channel change and historic mining sediments, *in* Gregory, K. J., ed., River channel changes: Chichester, United Kingdom, John Wiley, p. 353–368.

Marron, D. C., 1992, Floodplain storage of mine tailings in the Belle Fourche river system: A sediment budget approach: Earth Surface Processes and Landforms, v. 7, p. 675–685.

Meade, R. H., 1985, Suspended sediment in the Amazon River and its tributaries in Brazil during 1982–1984: U.S. Geological Survey Open-File Report 85–492, 39 p.

Meade, R. H., Nordin, C. F., Jr., Curtis, W. F., Rodrigues, F. M. C., do Vale, C. M., and Edmond, J. M., 1979,

Sediment loads in the Amazon River: Nature, v. 278, p. 161–163.
Meade, R. H., Dunne, T., Richey, J. E., Santos, U. de M., and Salati, E., 1985, Storage and remobilization of suspended sediment in the lower Amazon River of Brazil: Science, v. 228, p. 488–490.
Mertes, L. A. K., 1985, Floodplain development and sediment transport in the Solimões-Amazon River in Brazil, [Master's thesis]: Seattle, University of Washington, 108 p.
Mertes, L. A. K., 1990, Hydrology, hydraulics, sediment transport and geomorphology of the central Amazon floodplain [Ph.D. dissert.]: Seattle, University of Washington, 225 p.
Mertes, L. A. K., 1994, Rates of floodplain sedimentation on the central Amazon River: Geology, v. 22, p. 171–174.
Mertes, L. A. K., 1997, Description and significance of the perirheic zone on inundated floodplains: Water Resources Research, v. 33, p. 1749–1762.
Mertes, L. A. K., and Dunne, T., 1988, Morphology and construction of the Solimões-Amazon River floodplain, *in* Nittrouer, C. A., and DeMaster, D. J., eds., Proceedings of the Chapman Conference on the Fate of Particulate and Dissolved Components within the Amazon Dispersal System: River and Ocean: Washington, D.C., American Geophysical Union, p. 82–86.
Mertes, L. A. K., and Meade, R. H., 1985, Particle sizes of sands collected from the bed of the Amazon River and its tributaries during 1982–1984: U.S. Geological Survey Open-File Report 85–333, 16 p.
Mertes, L. A. K., Smith, M. O., and Adams, J. B., 1993, Estimating sediment concentrations in surface waters of the Amazon River wetlands from Landsat images: Remote Sensing of the Environment, v. 43, p. 282–301.
Mertes, L. A. K., Dunne, T., and Martinelli, L. A., 1996, Channel-floodplain geomorphology along the Solimões-Amazon River, Brazil: Geological Society of America Bulletin, v. 108, p. 1089–1107.
Nicholas, A. P., and Walling, D. E., 1996, The significance of particle aggregation in the overbank deposition of suspended sediment on river floodplains: Journal of Hydrology, v. 186, p. 277–295.
Nittrouer, C. A., Curtin, T. B., and Demaster, D. J., 1986, Concentration and flux of suspended sediment on the Amazon continental shelf: Continental Shelf Research, v. 6, p. 151–174.
Nittrouer, C. A., Kuehl, S. A., Sternberg, R. W., Figueiredo, A. G., Jr., and Faria, L. E. C., 1995, An introduction to the geological significance of sediment transport and accumulation on the Amazon continental shelf: Marine Geology, v. 125, p. 177–192.
Nordin, C. F., Jr., Meade, R. H., Curtis, W. F., Bosio, N. J., and Landim, P. M. B., 1980, Size distribution of Amazon River bed sediment: Nature, v. 286, p. 52–53.
Nunn, J., and Aires, J. R., 1988, Gravity anomalies and flexure of the lithosphere at the middle Amazon Basin, Brazil: Journal of Geophysical Research, v. 93, no. B1, p. 415–428.
Parker, G., Sawai, K., and Ikeda, S., 1982, Bend theory of river meanders, part 2: Nonlinear deformation of finite-amplitude bends: Journal of Fluid Mechanics, v. 162, p. 303–314.
Petri, S., and Fúlfaro, V. J., 1988, Geologia do Brasil: Editoria da Universidade de São Paulo, Biblioteca de Ciencias Naturais, v. 9, 631 p.
Radambrasil, 1972, Mosaico semicontrolado de radar: Rio de Janeiro, Ministerio das Minas e Energia, Departamento Nacional de Producão Mineral, scale 1:250 000.
Räsänen, M., Salo, J., Jungner, H., and Romero Pittman, L., 1990, Evolution of the western Amazon lowland relief: Impact of Andean foreland dynamics: Terra Nova, v. 2, p. 320–332.
Reineck, H-E., and Singh, I. B., 1980, Depositional sedimentary environments: Berlin, Springer-Verlag, 549 p.
Richey, J. E., Meade, R. H., Salati, E., Devol, A. H., Nordin, C. F., Jr., and Santos, U. de M., 1986, Water discharge and suspended sediment concentrations in the Amazon River: 1982–1984: Water Resources Research, v. 22, p. 756–764.
Richey, J. E., Deser, C., and Nobre, C., 1989a, Amazon River discharge and climate variability: 1903–1985: Science, v. 246, p. 101–103.
Richey, J. E., Mertes, L. A. K., Dunne, T., Victoria, R. L., Forsberg, B. R., Tancredi, C. N. S., and Oliveira, E., 1989b. Sources and routing of the Amazon River flood wave: Global Biogeochemical Cycles, v. 3., p. 191–204.
Schmidt, G. W., 1972, Amounts of suspended solids and dissolved substances in the middle reaches of the Amazon over the course of one year (August, 1969–July, 1970): Amazoniana, v. 3, p. 203–223.
Sioli, H., 1957, Sedimentation im Amazonasgebiet: Geologische Rundschau, v. 45, p. 608–633.
Stallard, R. F., and Martin, D. A., 1989, Settling properties of suspended sediment from the Mississippi River: Second National Symposium on Water Quality, Abstracts: U.S. Geological Survey Open-File Report 89–409, p. 96.
Sternberg, H. O., 1955, Seismicité et morphologie en Amazonie brésilienne: Annales de Géographie, v. 64, p. 97–105.
Tricart, J. F., 1977, Types de lits fluviaux en Amazonie brésilienne: Annales de Géographie, v. 86, p. 1–54.
Trimble, S. W., 1983, A sediment budget for Coon Creek Basin in the Driftless Area, Wisconsin, 1853–1977: American Journal of Science, v. 283, p. 454–474.
Vanoni, V. A., ed., 1975, Sedimentation engineering: New York, American Society of Civil Engineers, 745 p.
Yalin, M. S., 1963, An expression for bed-load transport: American Society of Civil Engineers, Journal of the Hydraulics Division, v. 89, HY3, p. 221–250.

MANUSCRIPT RECEIVED BY THE SOCIETY AUGUST 7, 1996
REVISED MANUSCRIPT RECEIVED JULY 21, 1997
MANUSCRIPT ACCEPTED AUGUST 27, 1997

Printed in U.S.A.